Methodologies to determine b-term coefficients revisited

Song, Huiying; Sadriaj, Donatela; Desmet, Gert; Cabooter, Deirdre

Published in:
Journal of Chromatography A

DOI:
10.1016/j.chroma.2017.11.070

Publication date:
2018

Methodologies to determine b-term coefficients revisited

Huiying Song[(1)], Donatela Sadriaj[(1)], Gert Desmet[(2)], Deirdre Cabooter[(1,*)]

[(1)]KU Leuven, Department for Pharmaceutical and Pharmacological Sciences, Pharmaceutical Analysis, Herestraat 49, Leuven, Belgium

[(2)]Vrije Universiteit Brussel, Department of Chemical Engineering, Pleinlaan 2, 1050 Brussel, Belgium

(*) corresponding author:

tel.: (+) 32 (0)16.32.34.42, fax: (+) 32 (0)16.32.34.48, e-mail:

deirdre.cabooter@kuleuven.be

Abstract

The accuracy of the longitudinal diffusion term (b-term) plays a vital role in the study of mass transfer mechanisms in high performance liquid chromatography (HPLC). In this study, three commonly used methodologies (peak parking; fitting of an experimental van Deemter curve; and the so-called dynamic method) for the determination of the b-term constant were investigated in detail. The three methods were compared based on their mutual agreement, the intra- and inter-day variation of the obtained values and the time required to measure them. Whereas the dynamic method was found to be plagued by impractically long waiting times and concomitant baseline variations compromising accurate measurements of the band broadening, the two other methods lead to very similar b-values, i.e., well within the 1% RSD inter-day variation typically marking both methods in the present study.

The best way to study the agreement of the peak parking and plate height fitting method is in a plot of h.ν versus ν, providing a much better zoom on the b-term region of the van Deemter curve than the customarily employed h versus ν-curve and hence allowing to identify any anomalous measurement values (usually related to measurements with a long experimentation time). Verifying the mutual agreement between both methods is proposed here as an additional accuracy check of the obtained data.

Keywords: longitudinal diffusion; b-term coefficient; peak parking; plate height models; dynamic method.

1. Introduction

In the past decades, column technology has evolved rapidly to meet the more challenging requirements of liquid chromatography users. Higher column efficiencies, better sample resolution and a far shorter analysis time are important requirements in modern day applications of chromatography. This has resulted in a significant progress in the design, manufacturing, and packing of narrow bore and short chromatographic columns with various types of packing materials. Columns packed with sub-2 µm or even nearly 1 µm particles and with lengths between 50 and 150 mm are nowadays commercially available [1–4]. These new column technologies have opened the way to faster and more efficient chromatographic separations. The resulting decrease in column permeability has been dealt with by the development of ultra-high pressure liquid chromatography equipment (UHPLC) able to operate at pressures up to 1500 bar [5–8]. As a compromise between column efficiency and permeability, column manufacturers have also successfully revived core-shell or superficially porous particles (sub-3 µm particle size), which provide a satisfactory sample loading capacity and allow fast separations and peak resolutions comparable with those of sub-2 µm fully porous particles without producing excessive backpressures [9,10].

The primary mechanical quality of a column is its efficiency, represented by the height equivalent to a theoretical plate height (HETP or H), which is mainly controlled by three independent and additive contributions: the dispersion due to the mobile phase velocity inequalities in the packed bed (a-term in the van Deemter equation), the dispersion due to the longitudinal diffusion (b-term in the van Deemter equation), and the resistance to the mass transfer of the solute from the moving mobile zone to the stationary phase zone and vice versa (c-term in the van Deemter equation) [11]. The present study focuses on the longitudinal diffusion (b-term), representing the sole source of dispersion which continues to go on when the flow is switched off. It encompasses the combined effect of the molecular species diffusion in the mobile zone (= zone outside particles) and in the stagnant mobile phase liquid inside the particles

with the diffusion they experience when being in the retained state. Variations in its value mainly depend on the latter two, commonly combined under the term intra-particle diffusion [12,13].

An exact knowledge of the b-term is important to study the packing quality of columns (with the b- and c-term known, these contributions can be subtracted, leaving only the a-term dispersion). The re-introduction of core-shell particles has also demonstrated that the contribution of the b-term to band broadening is more important than was previously assumed [14]. Given its strong dependency on the intra-particle diffusion, an exact determination of the b-term constant, and more precisely its main constituting factor (D_{eff}, see Eq. (3) further on), furthermore also allows to produce a good estimate of the intra-particle diffusion coefficient (D_{part}), which in turn needs to be known to calculate the stationary zone contribution to the c-term dispersion [14–19].

The b-term constant can be determined in the absence or in the presence of a flow [20]. The most obvious approach (given the definition of the b-term dispersion as the single remaining source of axial band broadening in the absence of a flow) is the measurement in the absence of a flow (static approach), most commonly referred to as peak parking [18–21] and originally introduced by Giddings and Knox [22]. The dynamic method (i.e., in the presence of a flow) is performed by recording the peak profile of a compound at the lowest possible flow rate. This approach is generally justified by the consideration that the contributions of the a- and c-term band broadening become vanishingly small at very low flow rates and can hence anyhow mostly be neglected such that it is not really necessary to switch off the flow completely. In a third approach, recently adopted by McCalley et al. [16], the somewhat cumbersome process of selecting an appropriately low flow rate has been replaced by determining the b-term constant by fitting experimentally recorded plate heights of a compound over a whole range of velocities using one of the many existing plate height models (i.e., van Deemter equation, Giddings equation, Knox equation) [15–17].

In the present study, the above mentioned three different b-term determination approaches have been investigated in detail using a large-volume Zorbax Eclipse Plus C18 column (4.6 × 250 mm, 5 µm), and acetophenone and 3'-methylacetophenone as test molecules. The mutual agreement, the intra- and inter-day variation and the time required to perform each of these approaches are evaluated and compared. The goal is to help the chromatographic community to choose an adequate b-term determination method based on their necessities (cf. the compromise between accuracy and precision versus the available time).

Although we opted to focus on the interstitial velocity-based b-term constant (to be used in combination with the interstitial velocity u_i), it goes without saying that all observations and conclusions also directly apply to the unretained marker velocity-based b-term constant (to be used in combination with the unretained marker velocity u_0). Given the definition of both velocities [23], the ratio between both b-term constants is simply equal to the ratio of the total over the external porosity of the bed ($u_i/u_0 = \varepsilon_T/\varepsilon$).

2. Experimental

2.1. Chemicals and Columns

HPLC grade acetonitrile (ACN) and tetrahydrofuran (THF) were purchased from Fisher Chemicals (Merelbeke, Belgium). Milli-Q water was prepared in the lab using a Milli-Q gradient water purification system from Millipore (Bedford, MA, USA). Acetophenone (99% pure) and 3'-methylacetophenone (98% pure) were obtained from Sigma-Aldrich (Steinheim, Germany). A set of 12 polystyrene standards with molecular weights ranging between 500 and 2,000,000 Da were purchased from Sigma-Aldrich (Bornem, Belgium). A Zorbax Eclipse Plus C18 column (4.6 × 250 mm, 5µm) was purchased from Agilent Technologies (Diegem, Belgium).

2.2. Apparatus

All band-broadening experiments, molecular diffusion coefficient measurements (D_m) and inverse size exclusion chromatography (ISEC) experiments were performed on an Agilent 1290 UHPLC system (Agilent Technologies, Waldbronn, Germany) with a pressure limit of 1200 bar (further referred to as "instrument A" in the text). The instrument consisted of a quaternary pump, autosampler and diode array detector (DAD) with a flow cell of 1 µL. Chemstation software (Agilent Technologies) was used for instrument control, data acquisition and processing. The overall system volume was experimentally determined to be 13.9 µL. The injection volume was 1 µL and the sampling rate was varied between 20 and 40 Hz, depending on the flow rate.

To measure molecular diffusion coefficients (D_m), PEEK tubing (vendor specifications: 0.20 inch × 50 feet) with a measured length of 1532 cm and a calibrated internal diameter (d_t) of 0.051709 cm was purchased from GRACE (Columbia, MD, USA). The tubing was coiled into a diameter (d_{coil}) of 24 cm for temperature control and calibrated by weighing the amount of water contained within it. A thermostatted water bath JULABO (Seelbach, Germany) was used to maintain the temperature at 30°C.

Peak parking experiments were performed on the previously described Agilent 1290 UHPLC system and additionally on an Ultimate 3000 HPLC system from Dionex Softron GmbH (further referred to as "instrument B" in the text) equipped with a high-pressure pump (LPG-3400A), autosampler (WPS-3000SL) and UV/VIS variable wavelength detector (VWD-3400) with a flow cell of 11 µL. The overall system volume was experimentally determined to be 20 µL. The sampling rate was set at 40 Hz. Chromeleon software version 6.80 (Thermo Scientific) was used for data acquisition and instrument control. The injection volume used for the peak parking experiments was 1 µL.

For all band broadening and peak parking experiments, the column temperature was kept constant at 30°C by using a Spark Mistral oven (Emmen, Netherlands). All

experiments were conducted using two pieces of Viper tubing with an I.D. of 75 µm and length of 550 mm (Thermo Scientific) between the injector and the inlet of the column, and the outlet of the column and the detector, respectively. For the ISEC experiments, the detection wavelength was set at 225 nm, for the other measurements, it was set at 254 nm.

All data were analyzed using the method of moments and at half the peak height, using the instruments' software. The latter data are shown in the supporting information.

2.3. Methodology

2.3.1. Sample and mobile phase preparation

Acetophenone and 3'-methylacetophenone were selected as the test molecules, since they were neutral and well-retained under the investigated conditions. For the band broadening and peak parking experiments, stock solutions of acetophenone and 3'-methylacetophenone were prepared in ACN, in a concentration of 3000 ppm and 4000 ppm, respectively. Fresh samples (acetophenone 300 ppm, 3'-methylacetophenone 320 ppm) were prepared daily by mixing and diluting stock solutions in the mobile phase. A set of twelve polystyrene standards (MW=500; 2,000; 3,000; 10,000; 20,000; 30,000; 70,000; 150,000; 300,000; 700,000; 1,000,000; 2,000,000) were used to perform ISEC experiments. Each standard was dissolved in THF at a concentration of 1 mg/mL.

For all plate height, peak parking and D_m measurements, the same batch of mobile phase was used with a composition of ACN/H_2O (45/55, v/v) leading to a zone retention factor of k"~ 2.8 for acetophenone and k"~ 4.7 for 3'-methylacetopheone. Figure 1 shows a representative chromatogram that was obtained at a flow rate of 1 mL/min, displaying narrow peaks with excellent peak shapes. Tetrahydrofuran was used as the mobile phase to perform the ISEC experiments.

2.3.2. Peak parking method

In this method, the analyte of interest was injected into the column at a flow rate of 0.5 mL/min. When the compound migrated approximately half way down the column, the flow was abruptly arrested for a given time (t_{park}= 1 min, 16 min, 31 min, 46 min, 61 min and 91 min). During this "parking time", the analyte could diffuse freely under static conditions. Afterwards, the flow was resumed and the analyte peak eluted from the column towards the detector. These measurements were repeated four times for each parking time.

According to Einstein's diffusion equation, the plot of the obtained peak variances (σ^2_x) of the sample band is a linear function of the applied peak parking time (t_{park}) [21,24]:

$$\sigma_x^2 = 2 \cdot D_{eff} \cdot t_{park} \quad (1)$$

The slope of this plot hence directly provides the value of the effective diffusion coefficient (D_{eff}) [13,14]. Bulk diffusion coefficients were measured at 30°C using the open tubular Taylor-Aris method wherein the variance (σ_t^2) and elution time (t) of a peak were measured after elution through a long, coiled capillary with diameter d_t at a low flow rate (0.1 mL/min) [25]:

$$D_m = \frac{d_t^2 \cdot t}{96 \cdot \sigma_t^2} \quad (2)$$

A low flow rate was applied to avoid secondary flow in the coiled capillary. The thus obtained molecular diffusion coefficients were $D_m = 1.19 \times 10^{-9}$ m^2/s for acetophenone and $D_m = 1.08 \times 10^{-9}$ m^2/s for 3'-methylacetophenone.

The reduced b-term coefficient was subsequently calculated from the experimentally determined values of D_{eff} and D_m as follows [14]:

$$b = 2\frac{D_{eff}}{D_m}(1 + k'') \quad (3)$$

Wherein the zone retention factor (k") is defined as (see Eq. 9 for u_i):

$$k'' = \frac{t_R \cdot L}{u_i} \quad (4)$$

To test the inter-day variation of the peak parking method, the peak parking measurements were repeated for each studied compound on two consecutive days using the same HPLC system, and on a third day using a completely different HPLC system (see § 2.2).

2.3.3. Plate height curve fitting method

2.3.3.1. Measurement of the plate height data

Plate height data were measured at 21 different velocities (ranging between 0.02 and 1.3 mL/min) in isocratic mode, in order to generate sufficient data points for a precise curve fitting. Measurements were performed in triplicate, by performing one injection at each flow rate starting from the lowest flow rate until all flow rates were evaluated, and then repeating this cycle two more times. During the plate height measurements, the accuracy of each flow rate was monitored by collecting the mobile phase at the outlet of the detector for a certain time. During the whole series of experiments, the column temperature was carefully monitored as well with a thermocouple (Fluke, Washington, United States) The observed temperature never deviated more than 0.2°C from the set temperature.

Peak variance (σ^2) and elution time (t_R) values were corrected for the system band broadening (σ^2_{sys}) and dead time (t_{sys}) [26]. The latter were determined by replacing the column with a zero dead-volume connector under the same experimental conditions as for the plate height measurements [27]. The system variance was less than 1.2% of the total variance of acetophenone, and less than 0.6% of the total variance of 3'-methyl acetophenone under all investigated conditions.

Plate counts (N) and plate heights (H) were subsequently calculated as follows:

$$N_{col} = \frac{\left(t_{R,total} - t_{R,sys}\right)^2}{\sigma^2_{total} - \sigma^2_{sys}} \quad (5)$$

$$H_{col} = \frac{L}{N_{col}} \quad (6)$$

Where L is the column length, the subscript "total" refers to the experimentally measured variance and analysis time and "col" refers to the pure column efficiency obtained after system correction.

Reduced plate heights (h) and reduced interstitial velocities (v_i) were calculated as:

$$h = \frac{Hcol}{d_p} \quad (7)$$

$$v_i = \frac{u_i \times d_p}{D_m} \quad (8)$$

With d_p the column particle size and u_i the interstitial velocity, determined as:

$$u_i = \frac{F}{\varepsilon_e \pi r^2} \quad (9)$$

Where ε_e is the external porosity and r is the column radius.

The external porosity (ε_e) was measured experimentally by inverse size exclusion chromatography (ISEC) using a set of twelve polystyrene standards [28]. The flow rate was set at 0.4 mL/min, and injection volumes were 1 µL. Each injection was performed in triplicate and the obtained retention volumes averaged. Retention volumes were corrected for the extra-column volume of the system. The elution volumes of the polystyrene standards were subsequently plotted against the cubic root of their molecular weights ($MW^{1/3}$). The external porosity was derived by extrapolating the exclusion branches of the ISEC plots to $MW^{1/3} = 0$ [29] and was determined to be 41.74% in this way.

2.3.3.2. Fitting of the plate height data

The b-term coefficients were determined by fitting the experimentally obtained plate height data to the following plate height models:

-van Deemter equation: $h = a + \frac{b}{v_i} + cv_i$ (10)

-Knox equation: $h = av_i^{1/3} + \frac{b}{v_i} + cv_i$ (11)

-free n-Knox equation: $h = av_i^n + \frac{b}{v_i} + cv_i$ (12)

-Giddings equation: $h = \left(\frac{1}{a} + \frac{1}{dv_i}\right)^{-1} + \frac{b}{v_i} + cv_i$ (13)

The fitting procedure was performed using the solver function of Microsoft Excel, using the GRG Nonlinear Solving engine (constraint precision: 0,000001, convergence: 0,0001 and population size: 100).

2.3.4. Dynamic method

In this method, the b-term coefficients were calculated based on the experimental plate height data obtained at very low flow rates, based on the assumption that the a- and c-terms are very small at these flow rates and therefore negligible:

$h \cong h_b = b \,/\, v \Rightarrow b \cong h \times v$ (14)

3. Results and Discussion

3.1. Peak parking method

Peak parking measurements were first performed on instrument A by determining peak variances (σ^2_x) at specific parking times. The obtained average values of $\Delta\sigma^2_x$ (out of four measurements per parking time) and their standard deviations shown as error bars as a function of the parking time are shown in Figure 2 (diamonds). Note that the standard deviations are so small, that they are hardly visible, indicating that the intra-day variability is negligible. To omit the effects of any possible variation in parking time, the data were plotted as a function of the actual parking time (calculated by subtracting the retention time of the peak when no parking time is applied from the retention time that is obtained when a certain parking time is applied). Note that the variances are reported as $\Delta\sigma^2_x$-values, obtained by subtracting the value for σ^2_x at t_{park}= 1 min from the variances at all subsequent parking times. From the slopes of the straight line relationship in Fig. 2, the effective diffusion coefficient D_{eff} was calculated according to Eq. (1), after which the b-term coefficient was calculated according to Eq. (3).

To assess the inter-day variability of the peak parking method, the same experiment was subsequently performed on the same instrument (instrument A), but on a second day, while the same experiment was also repeated on a third day, but now using a different HPLC system (instrument B), with a different system volume. The corresponding curves of $\Delta\sigma^2_x$ versus parking time have also been added to Figure 2 (squares and triangles). The average b-term values obtained from the slopes of the curves of $\Delta\sigma^2_x$ versus t_{park} by performing peak parking experiments on three different days were calculated to be b= 5.25 ± 0.06 for acetophenone, and b= 6.75 ± 0.03 for 3'-methyl acetophenone. Considering these data were measured on different days, using different instrumentation, the observed inter-day variability of maximum 1.1% can be considered to be very good.

To obtain a maximal insight in the generated data, the data in Figure 2 were subsequently replotted in Figure 3 by plotting $\Delta\sigma^2_x$ (1+k'')/(D_m.t_{park}) as a function of t_{park} to obtain a more zoomed-in view on the data. This approach is followed because it can be deduced from Eqs. (1) and (3) that the b-term values obtained at each individual parking time can also be directly calculated as follows:

$$b = \frac{\Delta\sigma_x^2}{t_{park}} \cdot \frac{(1+k'')}{D_m} \qquad (15)$$

The resulting b-term values (per individual parking time) are shown in Figure 3. A rather complex pattern can be observed, with some random variations between the different days (and instruments). The intra-day variability of the values obtained for the individual times (for four consecutive injections on the same day, represented by the error bars) was maximum 1.2%, while the inter-day variability (by performing the same experiments on three consecutive days and on two different instruments) was maximum 2.5%. The inter-day variability of the average values of the individual parking time values was much lower, resp. 0.6 and 0.7% for the two components (see Table 1).

To investigate some of the observed variations in more detail, the raw chromatograms obtained at different parking times were studied in more detail, but no anomalies or systematic changes could be found. All peaks were symmetrical at all parking times and all displayed a sufficiently large signal-to-noise ratio. This was confirmed by the fact that experiments performed at longer analysis times did not result in larger error bars, as can be deduced from Figure 3. Another potential source for the observed variation is the temperature at which the experiments were performed. However, all experiments were performed in a thermostatted oven compartment at 30.0°C of which the temperature was closely monitored and never deviated more than ±0.2°C. A clear explanation for the observed variation, which was anyhow limited, could therefore not be found. Note that similar variations were observed when the data were analyzed at half the peak heights, as can be seen in Figure S-2 in the Supporting Information.

Figure 3 also clearly shows that the variation obtained when performing the peak parking experiment on two different instruments is similar to or smaller than the variation obtained when performing the peak parking experiment on the same instrument, but on a different day. It can hence be concluded that the instruments themselves did not have any significant effect on the obtained b-term values. Similar observations were made when the data were analyzed at half the peak height (see Figure S-2 in the Supporting Information). The good agreement in slope values between the data analyzed at half the peak height and using the method of moments, moreover suggests a high symmetry of the obtained peaks.

3.2. Plate height curve fitting method

3.2.1. Measurement of the plate height data

Plate height curves were measured in triplicate by performing one injection per flow rate, from the lowest flow rate (set at 0.02 mL/min for practical reasons, see also further below) to the highest possible flow rate (limited by the maximum pressure of the column), and then repeating this cycle two additional times to investigate the maximum

possible variation in plate height. Since it took an entire day to measure one plate height curve, and each plate height curve was hence recorded at a different day, these measurements also immediately resulted in an assessment of the inter-day variability.

Figure 4 shows the average values of the plate heights that were obtained in this way for acetophenone (Figure 4a) and 3'-methylacetophenone (Figure 4b), respectively. The error bars represent the inter-day variability calculated as the RSD on the data. Figure S-3 in the Supporting Information shows the equivalent of this figure, but now relating to the peak width at half height. The accuracy of the flow rate was investigated by collecting the volume of mobile phase eluting from the column for the duration of the experiment at a specific flow rate (see section 2.3.3.1). The deviation between the set and measured flow rates was below 1% for all flow rates.

At the lowest flow rate of 0.02 mL/min, the inter-day variability on the plate height values amounted up to 4.8% for acetophenone and 11.6% for 3'-methylacetophenone. These high RSD values can most probably be directly related to the high degree of baseline drifting that was observed at this low flow rate (data not shown), which in turn can be directly explained by the very long analysis times (order of 10h!) associated with the measurement at this low flow rate. Baseline drifting can result in large errors in peak integration and peak height read-out and can hence strongly influence the accuracy of the measured plate heights. The plate height values obtained via the width at half the peak height showed a similar significant inter-day variability at the lowest flow rate, albeit slightly lower: 3.7% and 10.0% for acetophenone and 3'-methylacetophenone, respectively (see Figure S-3). Some baseline drifting was also observed at the other low flow rates of 0.025 and 0.030 mL/min, but the extent of this drifting was much smaller and only resulted in a plate height variation of 0.8% for acetophenone and 1.6% for 3'-methylacetophenone at 0.025 mL/min when analyzed using the method of moments. For all other flow rates, the variation in plate height values remained below 1% for both

393 compounds. These observations can also be directly made from the error bars added to
394 Figure 4 (and Figure S-3).
395
396 Baseline drift over the long measurement times associated with the very low flow rates
397 applied here are certainly not uncommon. One potential cause for this baseline drift
398 could be excluded as the column temperature was monitored carefully during all plate
399 height measurements and never deviated more than 0.2°C from the set temperature.
400 Other precautions (such as the prevention of the evaporation of solvents, manual
401 premixing and degassing of the mobile phase) were taken as well. A possible
402 explanation for the baseline drift could be small variations in the temperature of the
403 flow cell during the course of the longer analytical runs (at the lowest flow rates), since
404 the option to continuously heat the flow cell was not available.
405
406 3.2.2. Fitting of the plate height data
407 The measured plate heights were subsequently reduced into dimensionless coordinates
408 using Eqs. (7-8) and fitted to four plate height equations: the van Deemter, Knox, free
409 n-Knox and Giddings equation (see 2.3.3.2). The result is shown in Figure 5a for
410 acetophenone (analyzed using the method of moments). To assess which plate height
411 model fitted the experimentally obtained data best in the region of low velocities, the
412 original plate height data were replotted in such a way that a more zoomed-in view of
413 the data in this region was obtained (Fig. 5b). This was done by transforming the y-axis
414 from h to $h \cdot \nu_i$. As can be verified from any of the plate height models given in Eqs. (10-
415 13), this transformation leads to a curve that should directly converge to the value of b
416 when ν_i goes to zero. The $h \cdot \nu_i$-plot can moreover be very helpful to assess the quality
417 of the measured data and their fitting in the b-term regime, while the customarily used
418 h-plot does not give any clear detail. For the considered data set, the $h \cdot \nu_i$ -plot in Figure
419 5b for example readily reveals that the first two data points (at the lowest velocities)
420 are not in line with the other points at higher velocities and can hence be considered as
421 measurement outliers or artefacts, most probably related to the baseline drift problem

occurring at these low flow rates as discussed above. Fitting the plate height data including the first two data points lead to very poor quality fits with clearly inconsistent parameter values (data not shown). However, by omitting the first two data points from the fitting, as is shown in Figure 5b, excellent fits are obtained. Figure 5b also shows that very little difference in fitting quality is obtained when using either the Knox, the free n-Knox or the Giddings model. Given Knox himself eventually preferred the free n-Knox model (with n rather in the order of 0.5 to 1) over the more customarily used n=1/3-variant [30], and given the Knox-model can be seen as a practically useable approximation of the multi-scale Giddings model [22], we continued the rest of the study with the free n-Knox model. Fitting the data with the other models, the effect on the obtained b-values was however always very small (maximum variation in b-term value of 1%)

3.3. Dynamic method

The dynamic method consists of calculating the b-term coefficient from the plate height value measured at the lowest possible flow rate using Eq. (14). According to the specifications of the manufacturer, the instrument A used in this study can reach a minimum flow rate of 0.01 mL/min with great flow precision. In the current study, using well-retained compounds (k"= 4.66 for 3'-methylacetophenone), a flow rate of 0.01 mL/min would lead to an impractically large elution time, increasing the chance of baseline drifting. Therefore, a flow rate of 0.02 mL/min was chosen as the minimum flow rate.

As shown in Table 1 (bottom row), the b-term values obtained via Eq. (14) at this low flow rate are far off from all the other b-values, and furthermore display a very high inter-day variability. This should not be surprising, giving the flow rate used for the dynamic method is the same as the lowest flow rate in Figure 5, and hence suffers from the same baseline drift problem already discussed in the previous section.

Considering the accuracy of the method, yet another problem arises. Using any of the models represented by Eqs. (10-13) with typical values for a, b, c, d and n, it can be verified that the reduced velocities below which the a- and c-term contributions become less than 1% of the total plate height is of the order of ν_i=0.05-0.1. This is even less than the reduced velocity related to the lowest flow rate we could adopt in the present study. Taking into consideration the column particle size (d_p= 5 μm), column I.D. (4.6 mm), external porosity (ε_e= 41.7%), and molecular diffusion coefficients ($D_{m,acetophenone}$= 1.19×10^{-9} m^2/s and $D_{m,3'\text{-methyl acetophenone}}$= 1.08×10^{-9} m^2/s), the reduced interstitial velocities corresponding to the 0.02 mL/min flow rate are on the order of ν_i= 0.2 for both components, i.e. well above the ν_i=0.05-0.1 criterion, implying the dynamic method will never reach accurate values of the b-term coefficient.

3.4. Comparison of the different methods for the determination of the b-term coefficient

Figure 6 gives an overview of the different methods in a $h\cdot\nu_i$–plot. The open symbols added at ν_i=0 represent the values obtained with the peak parking method for the individual parking times (as shown in Figure 3). The two horizontal lines represent the average of these points (dashed line) and that derived from the slope in the $\Delta\sigma^2_x$ versus t_{park}-plots (solid line). The b-value corresponding to the lowest reduced velocity point (somewhere around ν_i= 0.2) also represents the value obtained with the dynamic method.

As can be noted, the $h\cdot\nu_i$–plots in Figure 6 are ideally suited to show that there is a very good agreement between the fitting method (at least when omitting the data points that are clearly off the trend of the other data points in the van Deemter curve; in this case the first two data points for acetophenone, and the first three data points for 3'-methyl acetophenone) and the peak parking method. The difference in b obtained via the fitting method and any of the two horizontal lines obtained via peak parking is not larger than

0.7%. Similar observations are also made for the data analyzed at half the peak height as can be seen in Figure S-5 in the Supporting Information.

Figure 6 also readily shows that the dynamic method can be discarded as a useful method. Similar conclusions can be drawn from Table 1, summarizing the b-term values obtained using three different methods of determination, together with their inter-day variability (hence the variation in b-term coefficient obtained by performing experiments on three different days). As can be noted, the maximum variation in b-term obtained by fitting the plate height data to the free n-Knox model and using the slope of the peak parking curves is 0.4% for acetophenone and 1.7% for 3'-methylacetophenone. Comparing these values to the average b-term values obtained for the individual parking times, this variation is maximum 1.1% for acetophenone and 0.3% for 3'-methylacetophenone.

Also indicated in Table 1 is the total time required for each of the methods. The calculated required time includes the actual run time (retention time × 1.125) and processing time (1 min per chromatogram). Considering the inter-day variability obtained by performing experiments on three consecutive days was around or below 1% for most experiments, it should suffice to perform each experiment only once to obtain b-term data with sufficient reliability. Therefore, the required measurement time was calculated assuming each individual experiment was only carried out once. For the b-term values determined at individual peak parking times, the time to perform an experiment with t_{park}= 1 min was also taken into consideration.

From Table 1, it can be deduced that the dynamic method can be performed relatively fast (determination time comparable to or even smaller than the entire time required to perform peak parking). However, as was already clear from Figure 6, the dynamic method will never lead to accurate values of the b-term coefficient. Peak parking experiments conducted at a single peak parking time can also already produce accurate

values of the b-term in very short times. Comparing the b-values obtained from the slopes of the curves of $\Delta\sigma^2_x$ versus t_{park} with the b-values obtained at the individual parking times, the maximum deviation is around 2%.

The time required to record and analyze all plate height data required for the curve fitting is 4-5 fold larger compared to the other methods. When performing column performance studies, however, information on the a- and c-term is usually also desired, in which case plate height data covering a larger range of flow velocities are anyhow required.

3.5. Implications for the determination of the a-term contribution

Considering the inter-day variability data reported in Table 1, it is now interesting to assess what the implications of a certain variation in b-term value will be for the further determination of column performance parameters. From the general plate height model:

$$h = h_{eddy} + \frac{2}{\nu_i}\frac{D_{eff}}{D_m}(1+k")\frac{\varepsilon_e}{1-\varepsilon_e} + \frac{2}{\alpha}\frac{k"^2}{(1+k")^2}\frac{\varepsilon_e}{1-\varepsilon_e}\frac{\nu_i}{Sh_m} + \frac{2}{\alpha}\frac{k"}{(1+k")^2}\frac{\nu_i}{Sh_{part}\frac{D_{part}}{D_m}} \quad (16)$$

wherein D_{part} is the intra-particle diffusion coefficient, α a geometrical constant and Sh_m and Sh_{part} are the Sherwood numbers relating to the mobile and the intra-particle zone, respectively, it is clear that the determination of the b-term coefficient (or D_{eff}) will have implications on different levels.

The first level is of course the determination of the contribution of longitudinal diffusion itself. But also the contribution of the mass transfer resistance in the stationary zone will be affected by the b-value because D_{part} directly depends on D_{eff} (see Eq. 3 for relation between b and D_{eff}) according to following equations:

$$\frac{D_{eff}}{D_m} = \frac{1}{\varepsilon_e(1+k")}\frac{1+2\beta_1(1-\varepsilon_e)-\varepsilon_e\zeta_2\beta_1^2}{1-\beta_1(1-\varepsilon_e)-\varepsilon_e\zeta_2\beta_1^2} \quad (17)$$

Wherein, ζ_2 is a geometrical three-point parameter [31], β_1 is the polarizability constant:

$$\beta_1 = \frac{\alpha_{part}-1}{\alpha_{part}+2} \quad (18)$$

and α_{part} is the relative particle permeability:

$$\alpha_{part} = \frac{\varepsilon_e k''}{1-\varepsilon_e}\frac{D_{part}}{D_m} \quad (19)$$

Following Eqs. (17-19), it can be calculated that a 1% deviation in b-term (and hence a 1% deviation in D_{eff}/D_m-value) will lead to a 1.7% variation in D_{part}/D_m-value and hence a 1.7% variation in h_{cs}-value. For higher variations in b-term values (cfr. Table 1), this variation in h_{cs}-term increases to 3.4% (2% variation in b-term) and 5.1% (3% variation in b-term).

Finally, also the determination of the eddy dispersion term (the first term in Eq. (16) will be largely affected by the determination of the b-term value. Customarily, the value of the a-term is determined by subtracting the b- and c-term contributions from the overall measured plate height value.

Figure 7 shows the eddy dispersion terms that were calculated in this way for acetophenone and 3'-methylacetophenone. Note that the individual contributions of the b-term, h_{cs}-term and h_{cm}-term were calculated according to Eq. (16), with α= 6, Sh_{part}= 10 and $Sh_m = \frac{1.09}{\varepsilon_e} \cdot (\varepsilon_e \cdot \nu_i)^{\frac{1}{3}}$ [32]. The dashed lines indicate the a-term contribution that would be obtained for a 1% and 2.5% deviation of the b-term, showing the huge impact such seemingly small variations on the b-term constant have on the observed a-term, especially in the low velocity range. For a 1% deviation in b-term, a variation in a-term ranging between 133% at ν_i= 0.20 and 11% at ν_i= 1.2 is obtained for acetophenone. Only when the reduced velocity exceeds ν_i= 6.0, the variation in a-term becomes smaller than 1%. For 3'-methylacetophenone, the observed variation in a-term is slightly lower, ranging between 10 and 50% for reduced velocities of ν_i= 0.22 and 1.6. For a deviation of 2.5% in b-term these numbers are higher, a maximum variation in a-term of 330% (acetophenone) and 125% (3'-methylacetophenone) are obtained, and the variation in a-term only becomes smaller than 1% once the velocity exceeds ν_i= 12 (acetophenone) and ν_i= 14.5 (3'-methylacetophenone).

4. Conclusions

The three main methodologies (peak parking, dynamic method, plate height curve fitting) for the determination of the longitudinal diffusion or b-term constant have been revisited on a large, 5 μm particle column, and using acetophenone and 3'-methylaceto-phenone as test molecules.

Carefully measuring the raw data, the peak parking and the plate height fitting method were found to be in excellent agreement. The difference between the two methods was less than 0.7%, i.e., smaller than the inter-day variability of the individual methods. The fitting method takes longer to execute, but when one is anyhow measuring a full van Deemter curve, the fitting method can produce an accurate b-term value without any additional effort.

For those analysts willing to spend maximum effort to pursue a maximal accuracy, it is proposed here to combine both methods and use the type of $h.\nu_i$-plots shown in Figure 5b and Figure 6 to study their convergence and eliminate anomalous measurement points. For what concerns the peak parking method, possible measurement anomalies can best be detected using the type of $\Delta\sigma^2_x(1+k'')/(D_m.t_{park})$-plots shown in Figure 3, whose y-axis furthermore provides a direct read-out of b. The plot also shows that good measurements of the b-constant can be obtained measuring at only one parking time (in fact two because also t= 1 min needs to be determined).

The dynamic method needs to be carried out at such low flow rates that it leads to impractical analysis times, which furthermore increase the likelihood of severe baseline drifts, which in turn leads to totally unreliable measurements. The plate height fitting method is also plagued by this problem if one tries to include velocity data points that are too small. This leads to the somewhat contradictory conclusion that the velocities used in the plate height curve should not be taken too small, whereas the b-constant is in theory best approached when the velocity tends to zero (or is zero).

595

596 Overall, it seems difficult to determine the b-term constant with an RSD below 1%.
597 Although this precision in itself should be considered to be very good, the remaining
598 uncertainty leads to a very high uncertainty on the precise course of the a-term velocity
599 dependence. For the present column, the 1% uncertainty on b leads to an uncertainty on
600 the a-term contribution above 100% at ν_i= 0.2 and around 10% at ν_i= 1. Overall, the
601 data show that even with an extreme accuracy of the b-term measurement, it is in
602 intrinsically nearly impossible to determine the exact velocity dependence of the a-term
603 contribution for all reduced velocities below ν_i= 5.

604

605

606 **5. References**

607 [1] A.C. Sanchez, G. Friedlander, S. Fekete, J. Anspach, D. Guillarme, M. Chitty, T.
608 Farkas, Pushing the performance limits of reversed-phase ultra high performance
609 liquid chromatography with 1.3 µm core–shell particles, J. Chromatogr. A. 1311
610 (2013) 90–97. doi:10.1016/j.chroma.2013.08.065.

611 [2] M. Catani, O.H. Ismail, A. Cavazzini, A. Ciogli, C. Villani, L. Pasti, C. Bergantin,
612 D. Cabooter, G. Desmet, F. Gasparrini, D.S. Bell, Rationale behind the optimum
613 efficiency of columns packed with new 1.9 µm fully porous particles of narrow
614 particle size distribution, J. Chromatogr. A. 1454 (2016) 78–85.
615 doi:10.1016/j.chroma.2016.05.037.

616 [3] F. Gritti, G. Guiochon, Rapid development of core – shell column technology :
617 Accurate measurements of the intrinsic column efficiency of narrow-bore
618 columns packed with 4.6 down to 1.3 µm superficially porous particles, J.
619 Chromatogr. A. 1333 (2014) 60–69. doi:10.1016/j.chroma.2014.01.061.

620 [4] L.E. Blue, J.W. Jorgenson, 1.1 µm superficially porous particles for liquid
621 chromatography . Part I : Synthesis and particle structure characterization, J.
622 Chromatogr. A. 1218 (2011) 7989–7995. doi:10.1016/j.chroma.2011.09.004.

623 [5] M.E. Swartz, B.J. Murphy, Ultra performance liquid chromatography:
624 tomorrow's HPLC technology today, Lab Plus Int. 18 (2004) 6–9.

625 [6] J.R. Mazzeo, U.D. Neue, M. Kele, R.S. Plumb, W. Corp, A new separation
626 technique takes advantage of sub-2-µm HPLC, Anal. Chem. 1 (2005) 460A–
627 467A.

628 [7] T.H. Walter, R.W. Andrews, Recent innovations in UHPLC columns and
629 instrumentation, TrAC - Trends Anal. Chem. 63 (2014) 14–20.
630 doi:10.1016/j.trac.2014.07.016.

631 [8] J. De Vos, K. Broeckhoven, S. Eeltink, Advances in Ultrahigh-Pressure Liquid
632 Chromatography Technology and System Design, Anal. Chem. 88 (2016) 262–
633 278. doi:10.1021/acs.analchem.5b04381.

634 [9] G. Guiochon, F. Gritti, Shell particles , trials , tribulations and triumphs, J.

635 Chromatogr. A. 1218 (2011) 1915–1938. doi:10.1016/j.chroma.2011.01.080.
636 [10] D. Cabooter, F. Lestremau, F. Lynen, P. Sandra, G. Desmet, Kinetic plot method
637 as a tool to design coupled column systems producing 100,000 theoretical plates
638 in the shortest possible time, J. Chromatogr. A. 1212 (2008) 23–34.
639 [11] U.D. Neue, HPLC Columns: Theory, Technology and Practice, Wiley-VCH,
640 New York, 1997.
641 [12] G. Desmet, K. Broeckhoven, J. De Smet, S. Deridder, G. V. Baron, P. Gzil, Errors
642 involved in the existing B-term expressions for the longitudinal diffusion in fully
643 porous chromatographic media. Part I: Computational data in ordered pillar
644 arrays and effective medium theory, J. Chromatogr. A. 1188 (2008) 171–188.
645 doi:10.1016/j.chroma.2008.02.018.
646 [13] K. Miyabe, Y. Matsumoto, G. Guiochon, Peak parking-moment analysis. A
647 strategy for the study of the mass-transfer kinetics in the stationary phase, Anal.
648 Chem. 79 (2007) 1970–1982. doi:10.1021/ac061321h.
649 [14] A. Liekens, J. Denayer, G. Desmet, Experimental investigation of the difference
650 in B-term dominated band broadening between fully porous and porous-shell
651 particles for liquid chromatography using the Effective Medium Theory, J.
652 Chromatogr. A. 1218 (2011) 4406–4416. doi:10.1016/j.chroma.2011.05.018.
653 [15] H. Song, G. Desmet, D. Cabooter, Evaluation of the Kinetic Performance
654 Differences between Hydrophilic-Interaction Liquid Chromatography and
655 Reversed-Phase Liquid Chromatography under Conditions of Identical Packing
656 Structure, Anal. Chem. 87 (2015) 12331–12339.
657 doi:10.1021/acs.analchem.5b03697.
658 [16] J.C. Heaton, X. Wang, W.E. Barber, S.M.C. Buckenmaier, D. V. McCalley,
659 Practical observations on the performance of bare silica in hydrophilic
660 interaction compared with C18 reversed-phase liquid chromatography, J.
661 Chromatogr. A. 1328 (2014) 7–15. doi:10.1016/j.chroma.2013.12.058.
662 [17] H. Song, G. Desmet, D. Cabooter, Assessment of intra-particle diffusion in
663 hydrophilic interaction liquid chromatography and reversed-phase liquid

chromatography under conditions of identical packing structure, J. Chromatogr. A. (2017). doi:10.1016/j.chroma.2017.06.068.

[18] F. Gritti, G. Guiochon, A protocol for the measurement of all the parameters of the mass transfer kinetics in columns used in liquid chromatography, J. Chromatogr. A. 1217 (2010) 5137–5151. doi:10.1016/j.chroma.2010.06.016.

[19] F. Gritti, G. Guiochon, Mass transfer mechanism in hydrophilic interaction chromatography, J. Chromatogr. A. 1302 (2013) 55–64. doi:10.1016/j.chroma.2013.06.001.

[20] F. Gritti, G. Guiochon, Mass transfer kinetics, band broadening and column efficiency, J. Chromatogr. A. 1221 (2012) 2–40. doi:10.1016/j.chroma.2011.04.058.

[21] J.H. Knox, H.P. Scott, B and C terms in the Van Deemter equation for liquid chromatography, J. Chromatogr. A. 282 (1983) 297–313. doi:doi: DOI: 10.1016/S0021-9673(00)91609-1.

[22] J.H. Knox, L. McLaren, A New Gas Chromatographic Method for Measuring Gaseous Diffusion Coefficients and Obstructive Factors, Anal. Chem. 36 (1964) 1477–1482.

[23] D. Cabooter, J. Billen, H. Terryn, F. Lynen, P. Sandra, G. Desmet, Detailed characterisation of the flow resistance of commercial sub-2 ??m reversed-phase columns, J. Chromatogr. A. 1178 (2008) 108–117.

[24] F. Gritti, G. Guiochon, Effect of the surface coverage of C18 -bonded silica particles on the obstructive factor and intraparticle diffusion mechanism, Chem. Eng. Sci. 61 (2006) 7636–7650. doi:10.1016/j.ces.2006.08.070.

[25] J. Li, P.W. Carr, Accuracy of empirical correlations for estimating diffusion coefficients in aqueous organic mixtures., Anal. Chem. 69 (1997) 2530–2536. doi:doi: 10.1021/ac961005a.

[26] F. Gritti, G. Guiochon, Accurate measurements of peak variances : Importance of this accuracy in the determination of the true corrected plate heights of chromatographic columns, J. Chromatogr. A. 1218 (2011) 4452–4461.

693 doi:10.1016/j.chroma.2011.05.035.
694 [27] D. Guillarme, S. Heinisch, J.L. Rocca, Effect of temperature in reversed phase
695 liquid chromatography, J. Chromatogr. A. 1052 (2004) 39–51.
696 doi:10.1016/j.chroma.2004.08.052.
697 [28] H. Guan, G. Guiochon, Study of Physico-chemical properties of some packing
698 materials. I Measurements od the external porosity of packed columns by
699 inverswe size-exclusion chromatography., J. Chromatogr. A. 731 (1996) 27–40.
700 [29] F. Gritti, G. Guiochon, Speed-resolution properties of columns packed with new
701 4.6μm Kinetex-C18 core-shell particles, J. Chromatogr. A. 1280 (2013) 35–50.
702 doi:10.1016/j.chroma.2013.01.022.
703 [30] J.H. Knox, Band dispersion in chromatography — a universal expression for the
704 contribution from the mobile zone, J. Chromatogr. 960 (2002) 7–18.
705 [31] S. Deridder, G. Desmet, Calculation of the geometrical three-point parameter
706 constant appearing in the second order accurate effective medium theory
707 expression for the B-term diffusion coefficient in fully porous and porous-shell
708 random sphere packings, J. Chromatogr. A. 1223 (2012) 35–40.
709 doi:10.1016/j.chroma.2011.12.004.
710 [32] G. Desmet, K. Broeckhoven, Equivalence of the different Cm- and Cs- term
711 expressions used in liquid chromatography and a geometrical model uniting
712 them, Anal. Chem. 80 (2008) 8076–8088.

713

714

715 **6. Acknowledgements**

716 Agilent Technologies is kindly acknowledged for the gift of the Infinity 1290 system
717 through a University Relations Grant. Huiying Song acknowledges KU Leuven for
718 the post-doctoral mandate (PDM).

7. Figure Captions

Figure 1: Representative chromatogram of acetophenone (k"= 2.81) and 3'-methyl acetophenone (k"= 4.66) obtained on a Zorbax Eclipse Plus C18 column (4.6 × 250 mm, d_p= 5μm) at a flow rate of 1 mL/min. Mobile phase is ACN/H_2O (45/55, v/v).

Figure 2: Curves of $\Delta\sigma_x^2$ versus parking time (t_{park}) for **(a)** acetophenone and **(b)** 3'-methylacetophenone on (♦) instrument A on day 1, (▲) instrument A on day 2, and (■) instrument B on day 3. Error bars indicate the standard variations obtained by performing the same experiment four times consecutively on the same day. Data analyzed using the method of moments. The equations of the regression curves best fitting the experimental data are also given.

Figure 3: $\Delta\sigma_x^2/(2\cdot t_{park})$-data versus t_{park} representation of the data shown in Figure 2 for **(a)** acetophenone and **(b)** 3'-methylacetophenone on (♦) instrument A on day 1, (▲) instrument A on day 2, and (■) instrument B on day 3. Error bars indicate the standard variations obtained by performing the same experiment four times consecutively on the same day. Connecting lines have been added with the sole purpose of guiding the eye.

Figure 4: Curves of plate height (H) versus interstitial velocity (u_i) for **(a)** acetophenone and **(b)** 3'-methylacetophenone. The displayed data are the average values obtained for three measurements on three different days. Standard deviations on these values are shown as error bars. Data analyzed using the method of moments.

Figure 5: **(a)** Curves of h versus ν_i and **(b)** $h\cdot\nu_i$ versus ν_i for acetophenone. The symbols indicate the raw plate height data, the lines are the fitted curves obtained by fitting the experimental data to one of following plate height models: ( ) van Deemter, ( ) Knox, (- - -) free Knox, ( ) Giddings.

Figure 6: Curves of $h\cdot\nu_i$ versus ν_i for **(a)** acetophenone and **(b)** 3'-methylacetophenone

748 for experimental plate height data analyzed via the method of moments. Experimental
749 plate height data were fitted using the free Knox model by omitting the anomalous data
750 points for fitting as explained in the text. The horizontal lines represent the b-term
751 values obtained from the slope of the peak parking experiments ( ) and from the
752 average of the individual peak parking data ( ). The b-term values obtained for the
753 individual peak parking experiments are shown by the open symbols on the y-axis (◊
754 t_{park}= 15 min, ○ t_{park}= 30 min, □ t_{park}= 45 min, Δ t_{park}= 60 min and × t_{park}= 90 min). To
755 help interpret the precision, he double arrow on the y-axis indicates a 1% variation
756 (RSD) in b-term value.
757
758 **Figure 7:** Curves of h_a versus ν_i for **(a)** acetophenone (♦) and **(b)** 3'-
759 methylacetophenone. The a-term contribution is calculated by subtracting the b-, h_{cs}-
760 and h_{cm}- term from the overall plate height. The dashed lines indicate the a-terms that
761 would be obtained when the b-term would vary with 1% (----) or 2,5% (– –).
762

Figure 1

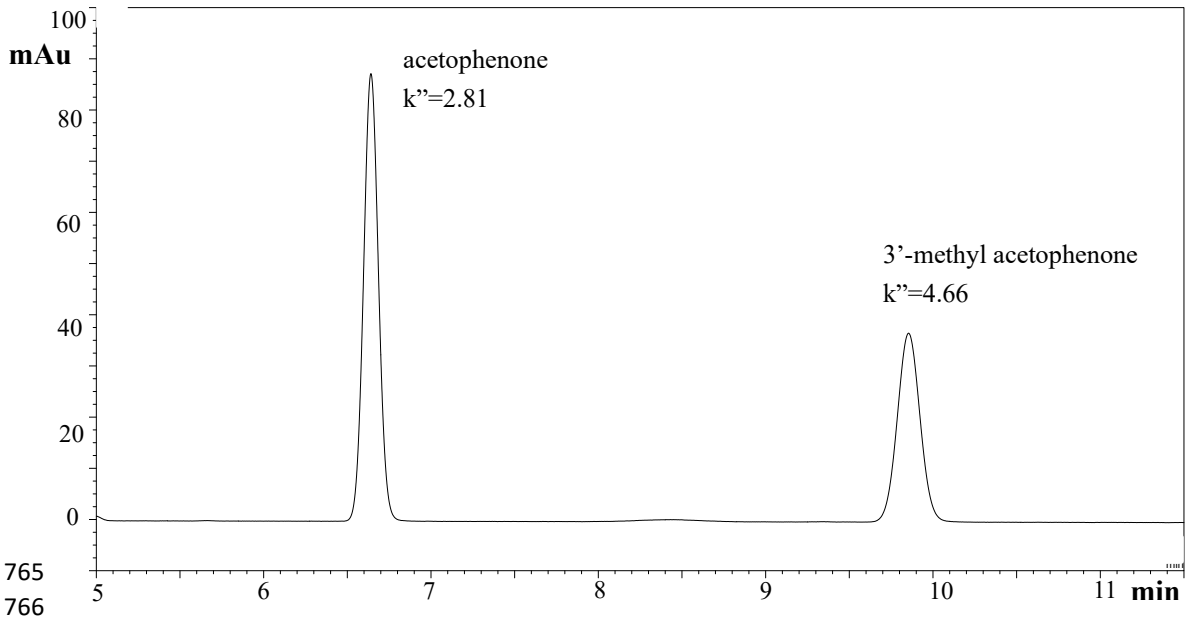
100
mAu
80
60
40
20
0
acetophenone
k"=2.81
3'-methyl acetophenone
k"=4.66
5
6
7
8
9
10
11
min

Figure 2

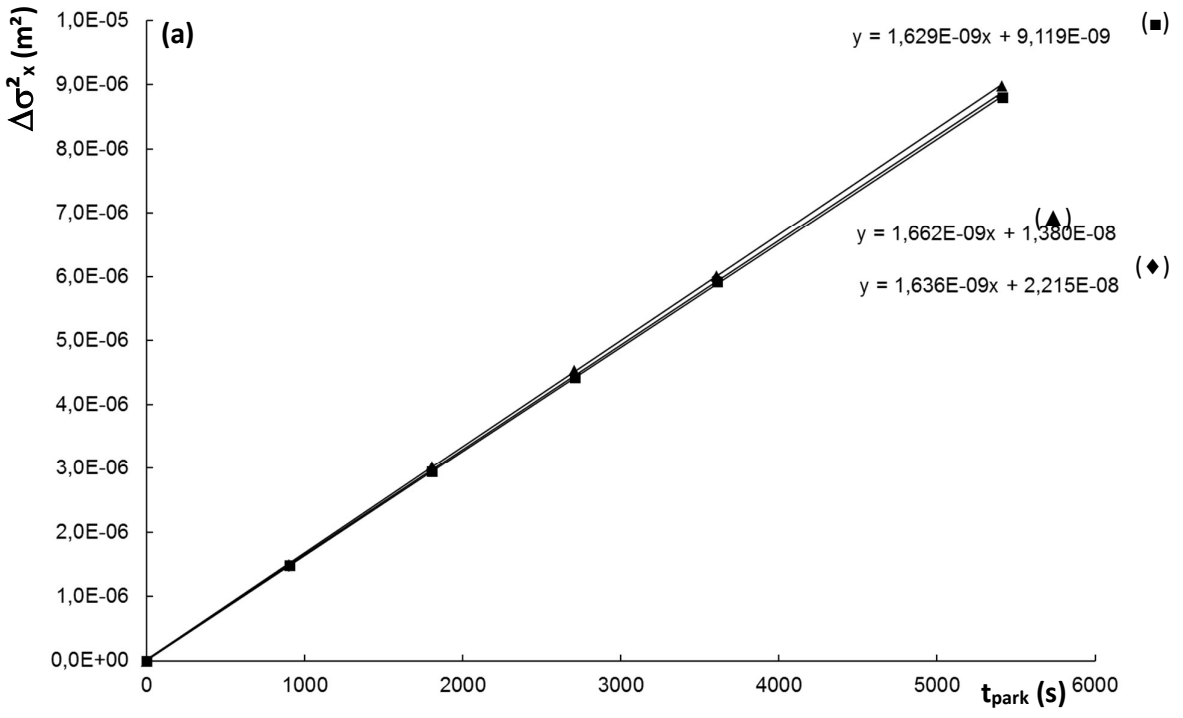
(a)
$\Delta\sigma^2_x$ (m²)
1,0E-05
9,0E-06
8,0E-06
7,0E-06
6,0E-06
5,0E-06
4,0E-06
3,0E-06
2,0E-06
1,0E-06
0,0E+00
0
1000
2000
3000
4000
5000
6000
t_{park} (s)
y = 1,629E-09x + 9,119E-09 (■)
y = 1,662E-09x + 1,380E-08 (▲)
y = 1,636E-09x + 2,215E-08 (♦)

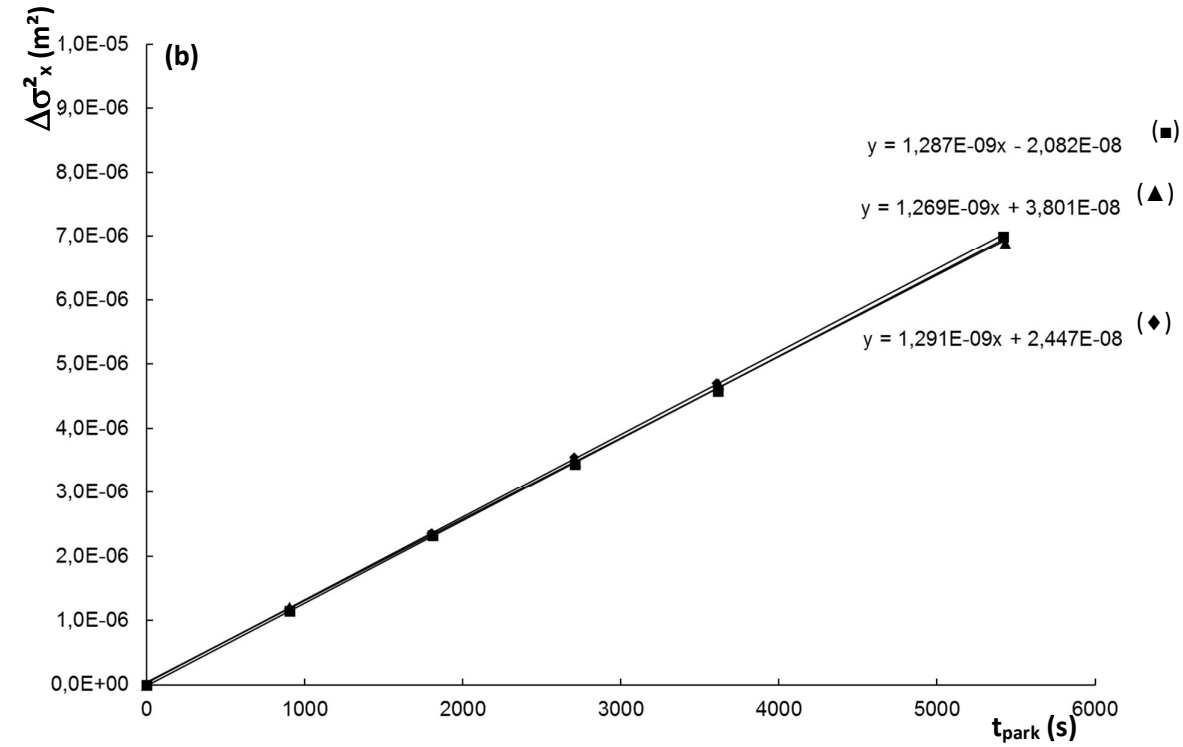
(b)
$\Delta\sigma^2_x$ (m²)
1,0E-05
9,0E-06
8,0E-06
7,0E-06
6,0E-06
5,0E-06
4,0E-06
3,0E-06
2,0E-06
1,0E-06
0,0E+00
0
1000
2000
3000
4000
5000
6000
t_{park} (s)
y = 1,287E-09x - 2,082E-08 (■)
y = 1,269E-09x + 3,801E-08 (▲)
y = 1,291E-09x + 2,447E-08 (♦)

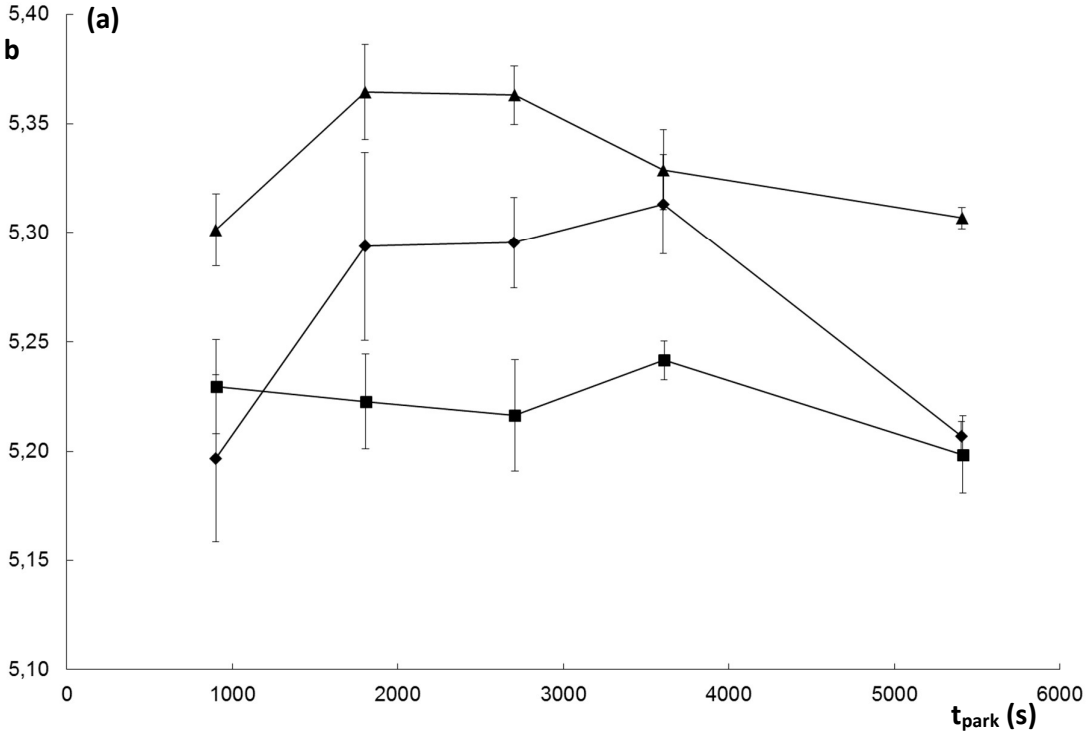
(a)
b
5,40
5,35
5,30
5,25
5,20
5,15
5,10
0
1000
2000
3000
4000
5000
6000
tpark (s)

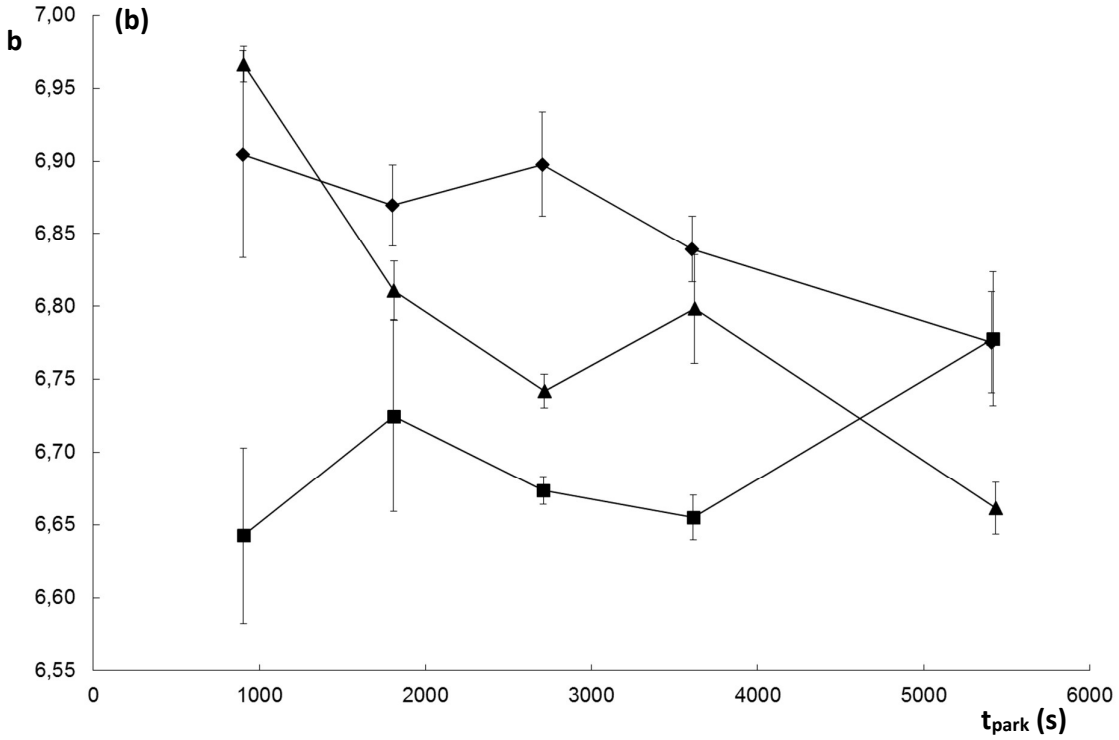
(b)
b
7,00
6,95
6,90
6,85
6,80
6,75
6,70
6,65
6,60
6,55
0
1000
2000
3000
4000
5000
6000
tpark (s)

Figure 3

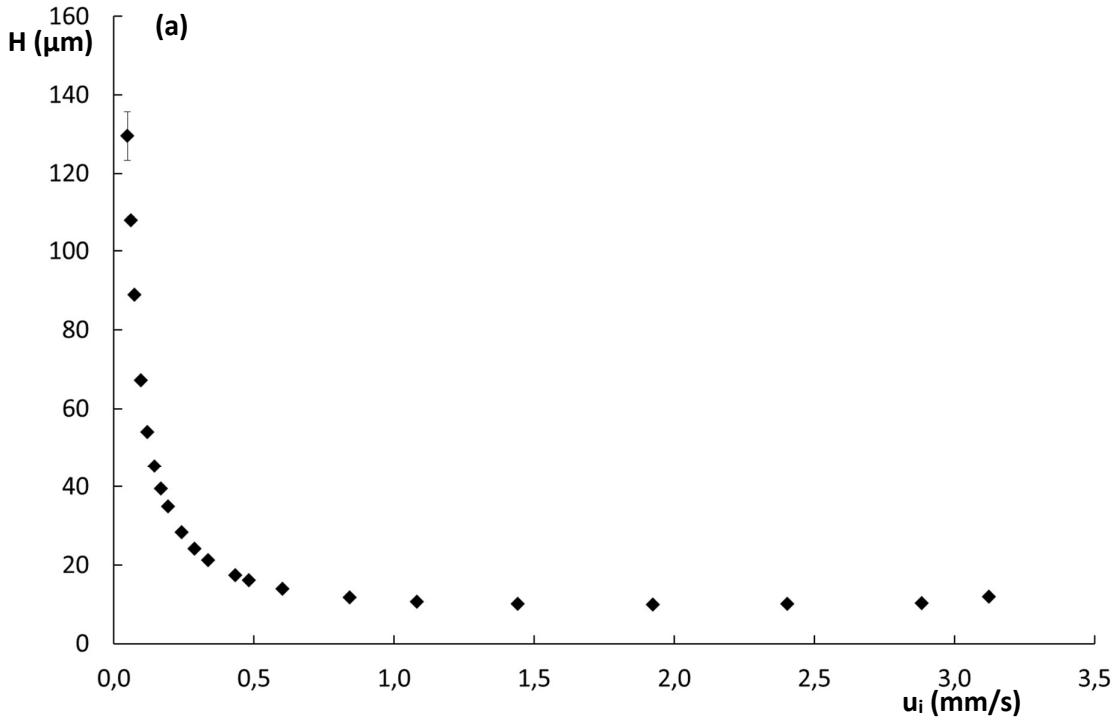
(a)
H (µm)
160
140
120
100
80
60
40
20
0
0,0
0,5
1,0
1,5
2,0
2,5
3,0
3,5
ui (mm/s)

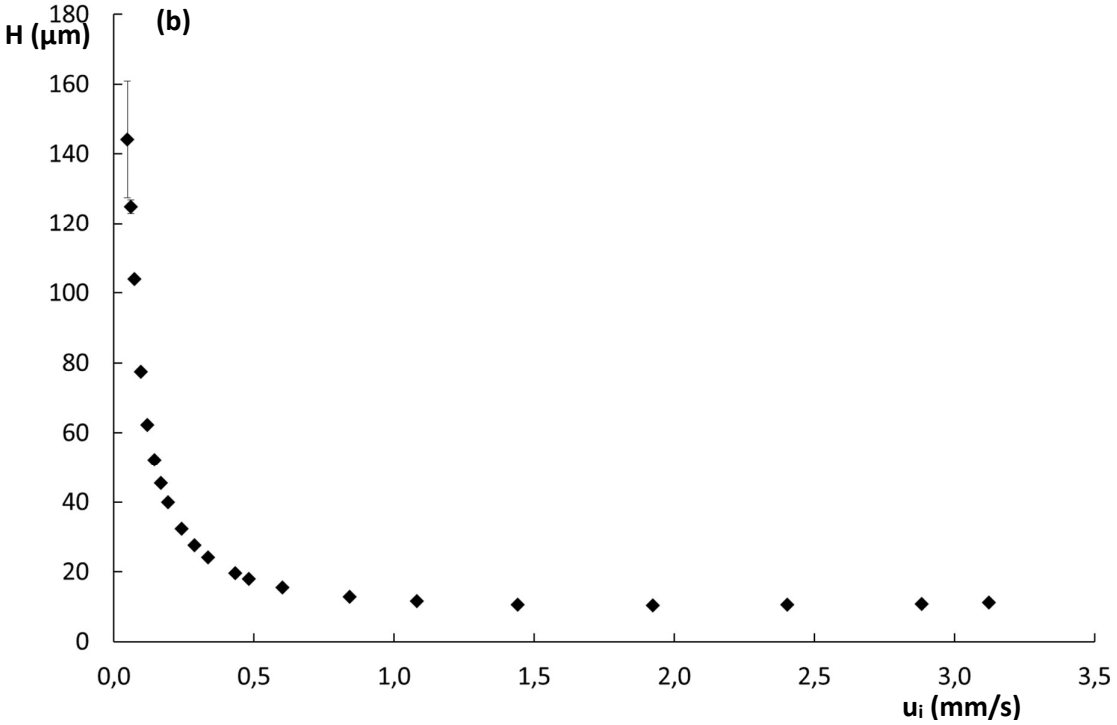
(b)
H (µm)
180
160
140
120
100
80
60
40
20
0
0,0
0,5
1,0
1,5
2,0
2,5
3,0
3,5
ui (mm/s)

Figure 4

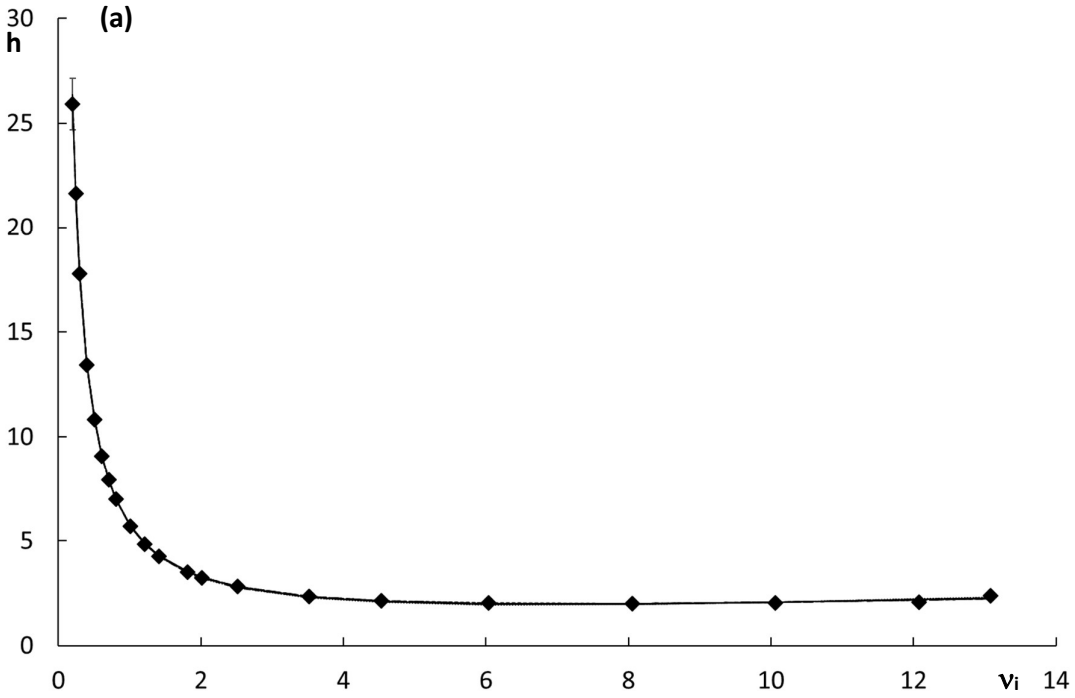
(a)
h
30
25
20
15
10
5
0
0
2
4
6
8
10
12
14
νi

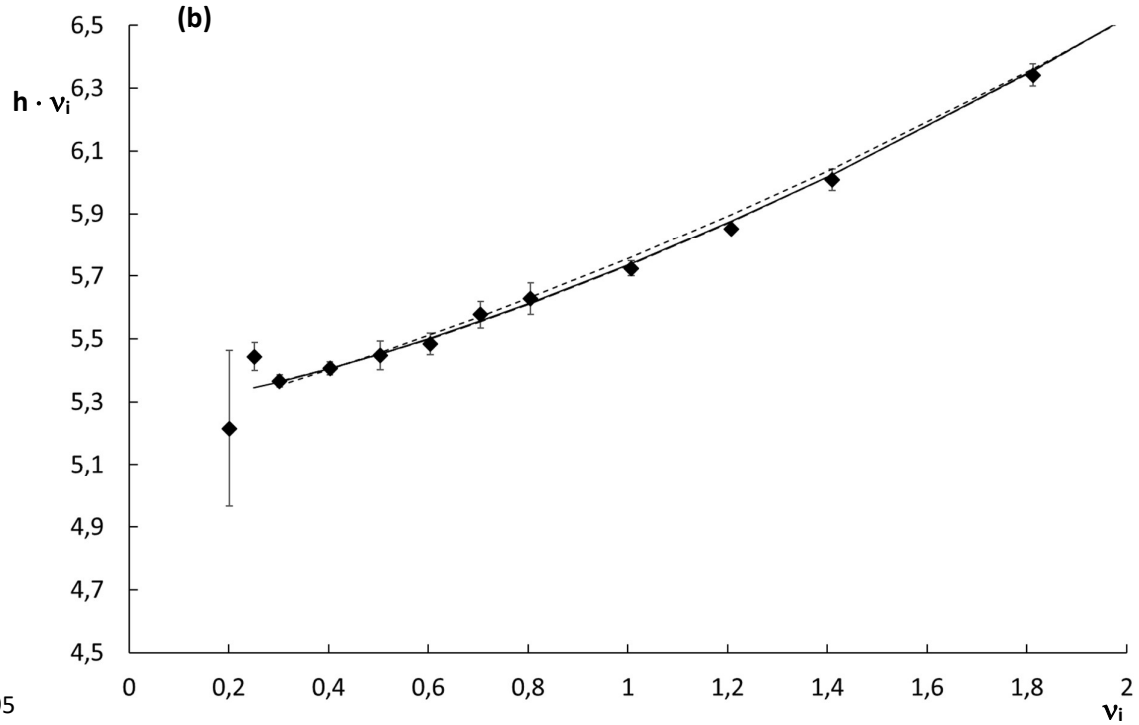
(b)
h · νi
6,5
6,3
6,1
5,9
5,7
5,5
5,3
5,1
4,9
4,7
4,5
0
0,2
0,4
0,6
0,8
1
1,2
1,4
1,6
1,8
2
νi

Figure 5

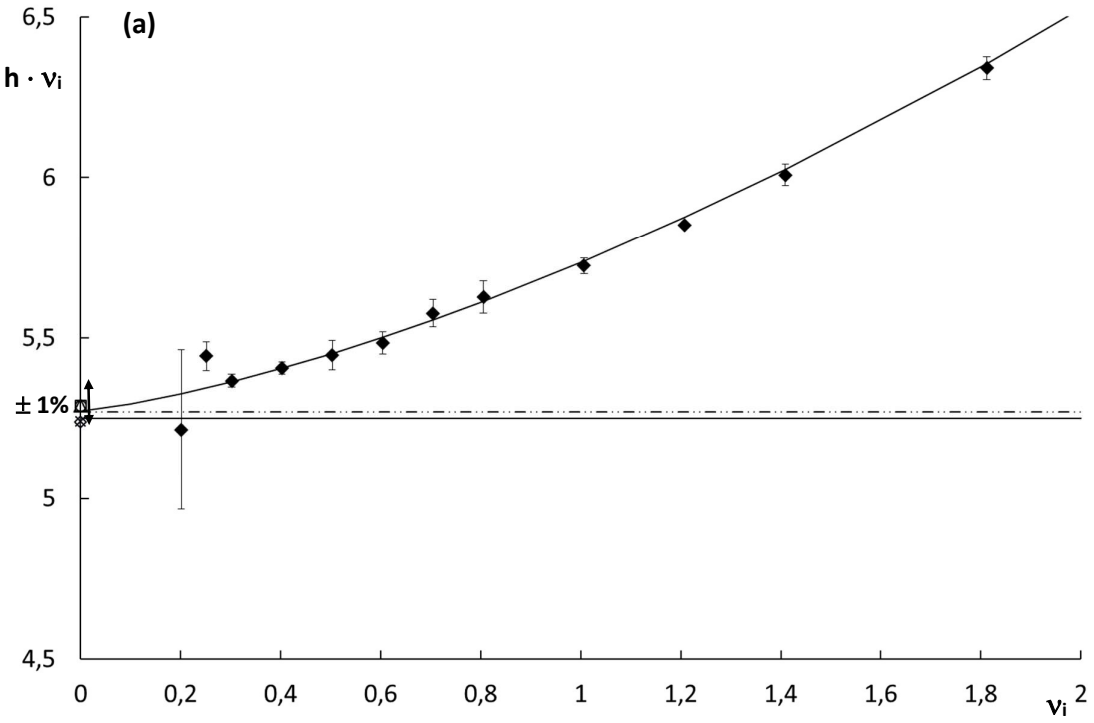
(a)
h · νi
6,5
6
5,5
5
4,5
± 1%
0
0,2
0,4
0,6
0,8
1
1,2
1,4
1,6
1,8
2
νi

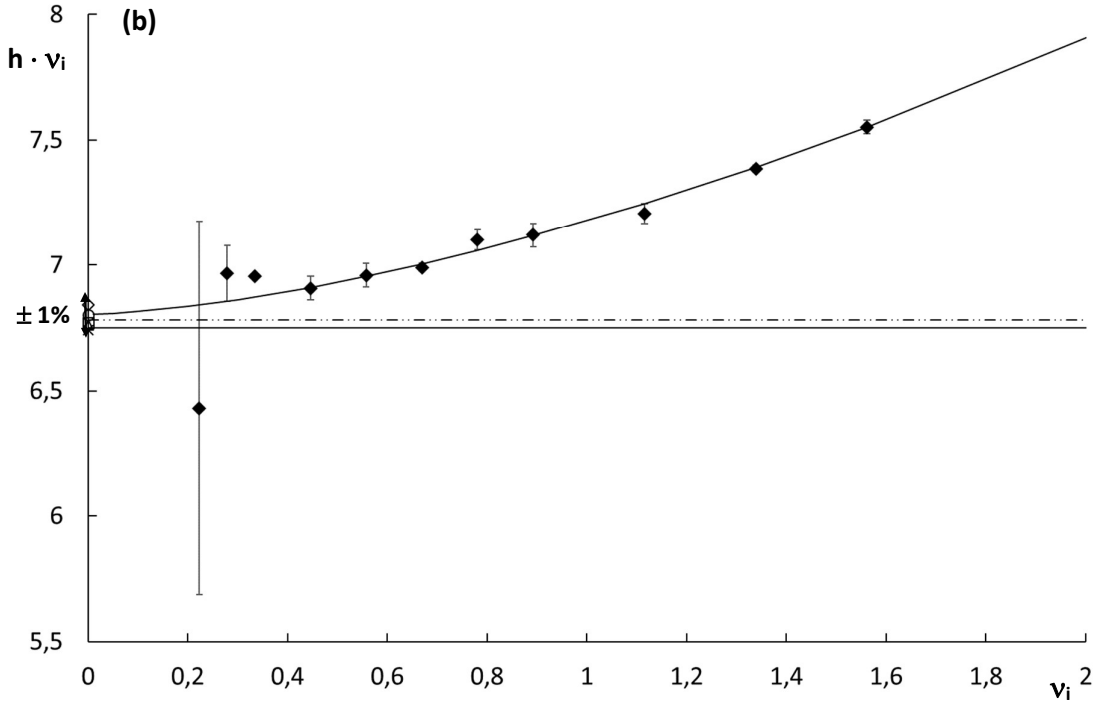
(b)
h · νi
8
7,5
7
6,5
6
5,5
± 1%
0
0,2
0,4
0,6
0,8
1
1,2
1,4
1,6
1,8
2
νi

Figure 6

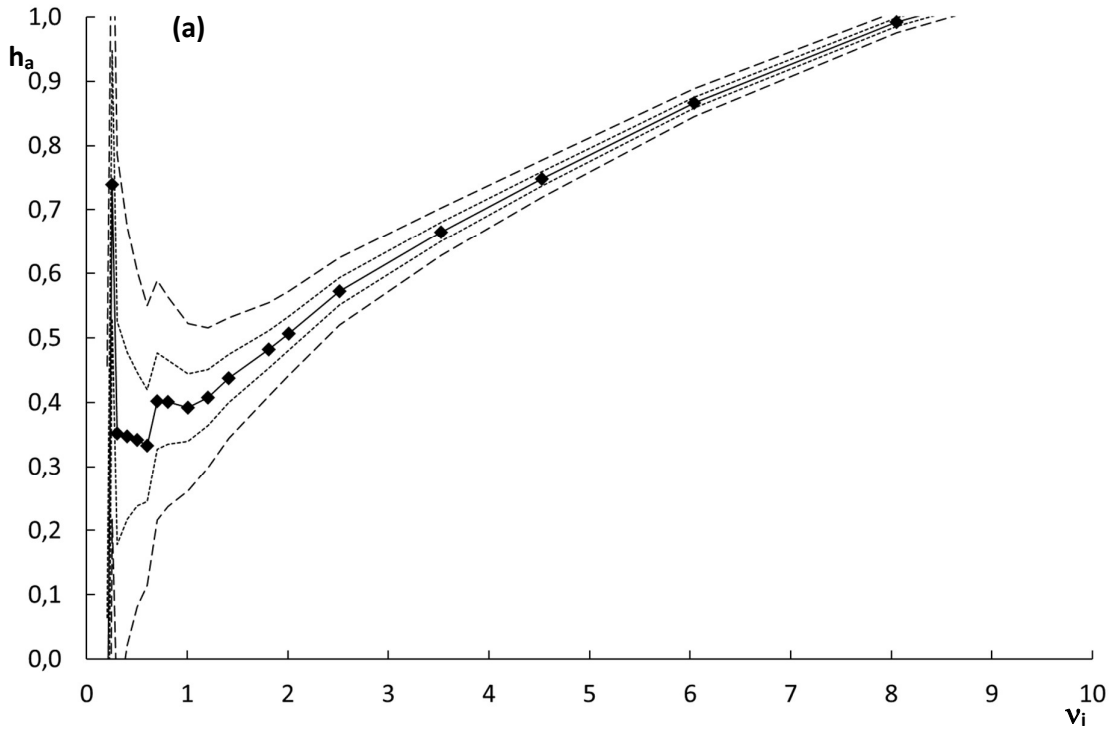
(a)
h_a
1,0
0,9
0,8
0,7
0,6
0,5
0,4
0,3
0,2
0,1
0,0
0
1
2
3
4
5
6
7
8
9
10
ν_i

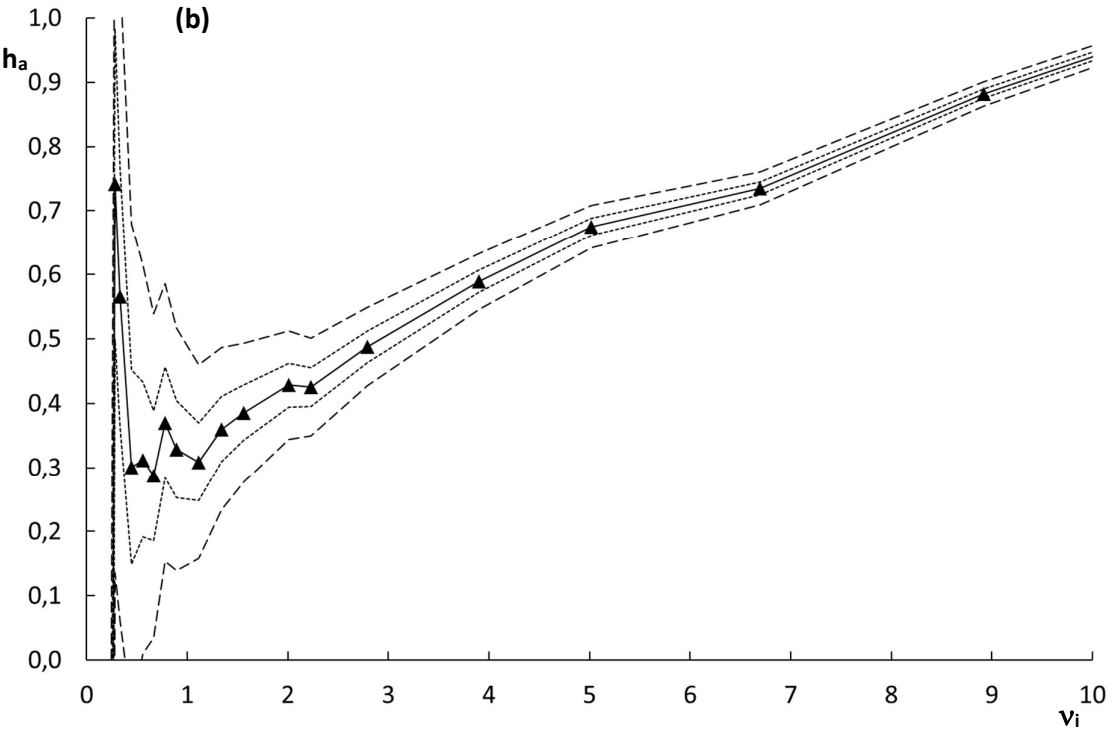
(b)
h_a
1,0
0,9
0,8
0,7
0,6
0,5
0,4
0,3
0,2
0,1
0,0
0
1
2
3
4
5
6
7
8
9
10
ν_i

Figure 7

817

818

3'-methylacetophenone					
method of determination		required time (min)	method of moments		half h
			b	RSD (%)	b
peak parking	slope	417	6,75	0,5	6,66
	t_{park} = 15 min	66	6,84	2,5	6,88
	t_{park} = 30 min	83	6,80	1,1	6,83
	t_{park} = 45 min	100	6,77	1,7	6,78
	t_{park} = 60 min	117	6,76	1,4	6,74
	t_{park} = 90 min	150	6,74	1,0	6,66
	average individual t_{park}	417	6,78	1,5	6,78
curve fitting*	Van Deemter	2927	6,67	0,6	6,64
	Knox	2927	6,77	0,5	6,75
	Free Knox	2927	6,80	0,6	6,77
	Giddings	2927	6,84	0,6	6,80
dynamic method	ν_i= 0,22	567	6,43	11,5	6,57

819

820 * curve fitting performed by omitting the first 3 data points.

821

822

823

Supporting Information

Methodologies to determine b-term coefficients revisited

Huiying Song[(1)], Donatela Sadriaj[(1)], Gert Desmet[(2)], Deirdre Cabooter[(1,*)]

[(1)]KU Leuven, Department for Pharmaceutical and Pharmacological Sciences, Pharmaceutical Analysis, Herestraat 49, Leuven, Belgium

[(2)]Vrije Universiteit Brussel, Department of Chemical Engineering, Pleinlaan 2, 1050 Brussel, Belgium

(*) corresponding author:

tel.: (+) 32 (0)16.32.34.42, fax: (+) 32 (0)16.32.34.48, e-mail: deirdre.cabooter@kuleuven.be

Abstract

The Supporting Information supplies a number of figures that were obtained by analyzing the data represented in the original manuscript at half the peak height.

Table of contents

Figure S-1: Curves of $\Delta\sigma_x^2$ versus parking time (t_{park}) for **(a)** acetophenone and **(b)** 3'-methylacetophenone on (♦) an Infinity 1290 UHPLC instrument on day 1, (▲) an Infinity 1290 UHPLC instrument on day 2, and (■) an Ultimate 3000 HPLC instrument on day 3.

Figure S-2: Curves of $\Delta\sigma_x^2/(2 \cdot t_{park})$ versus t_{park} for **(a)** acetophenone and **(b)** 3'-methylacetophenone on (♦) an Infinity 1290 UHPLC instrument on day 1, (▲) an Infinity 1290 UHPLC instrument on day 2, and (■) an Ultimate 3000 HPLC instrument on day 3.

Figure S-3: Curves of plate height (H) versus interstitial velocity (u_i) for **(a)** acetophenone and **(b)** 3'-methylacetophenone. The displayed data are the average values obtained for three measurements on three different days.

Figure S-4: Curves of $h \cdot \nu_i$ versus ν_i for acetophenone analyzed at half the peak height. The symbols indicate the raw plate height data, the lines are the fitted curves obtained by fitting the experimental data to one of following plate height models: ( ) van Deemter, ( ) Knox, ( ) free Knox, ( ) Giddings. The first two data points were omitted for the curve fitting.

Figure S-5: Curves of $h \cdot \nu_i$ versus ν_i for (a) acetophenone and (b) 3'-methylacetophenone for experimental plate height data analyzed at half the peak height. Experimental plate height data were fitted using the free n-Knox model by omitting the first two datapoints ( ). The horizontal lines represent the b-term values obtained

from the slope of the peak parking experiments ( ) and from the average of the individual peak parking data ( ). The b-term values obtained for the individual peak parking experiments are shown by the open symbols on the y-axis (◊ t_{park}= 15 min, ○ t_{park}= 30 min, □ t_{park}= 45 min, Δ t_{park}= 60 min and × t_{park}= 90 min).

880 **Figure S-1:** Curves of $\Delta\sigma_x^2$ versus parking time (t_{park}) for **(a)** acetophenone and **(b)** 3'-
881 methylacetophenone on (♦) an Infinity 1290 UHPLC instrument on day 1, (▲) an
882 Infinity 1290 UHPLC instrument on day 2, and (■) an Ultimate 3000 HPLC instrument
883 on day 3. Error bars indicate the standard variations obtained by performing the same
884 experiment four times consecutively. Data analyzed at half the peak height.
885

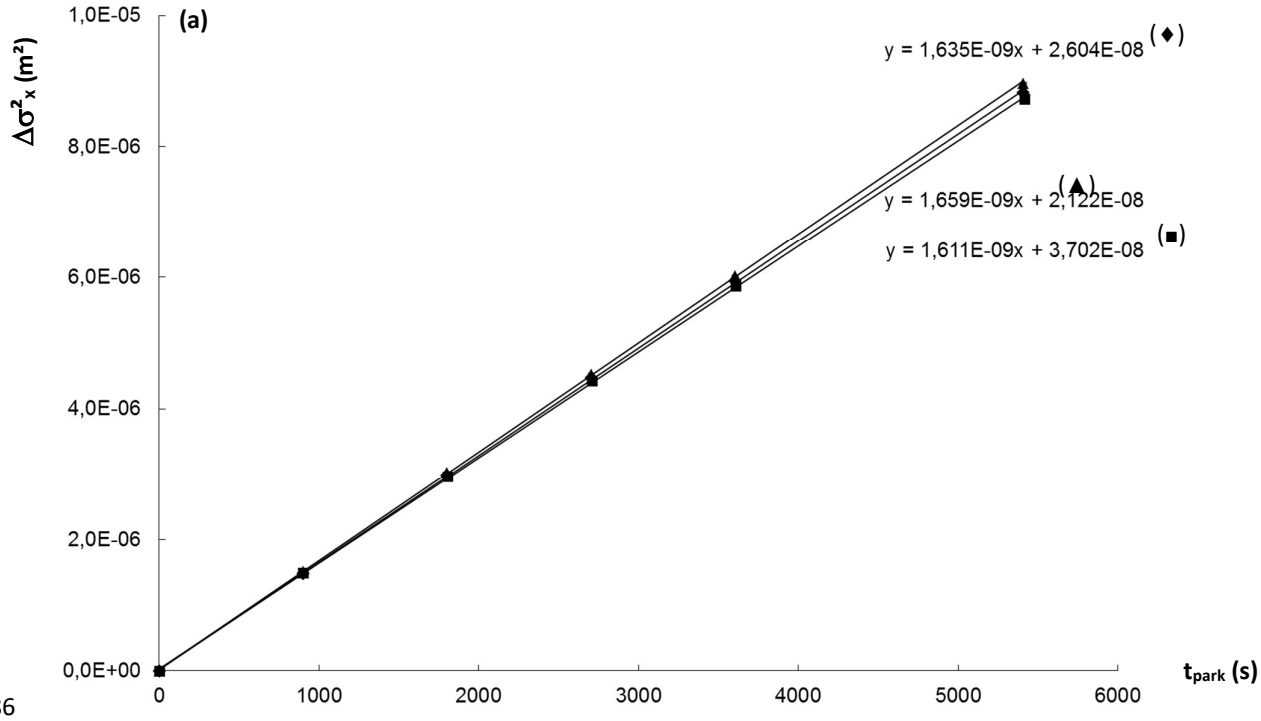

886

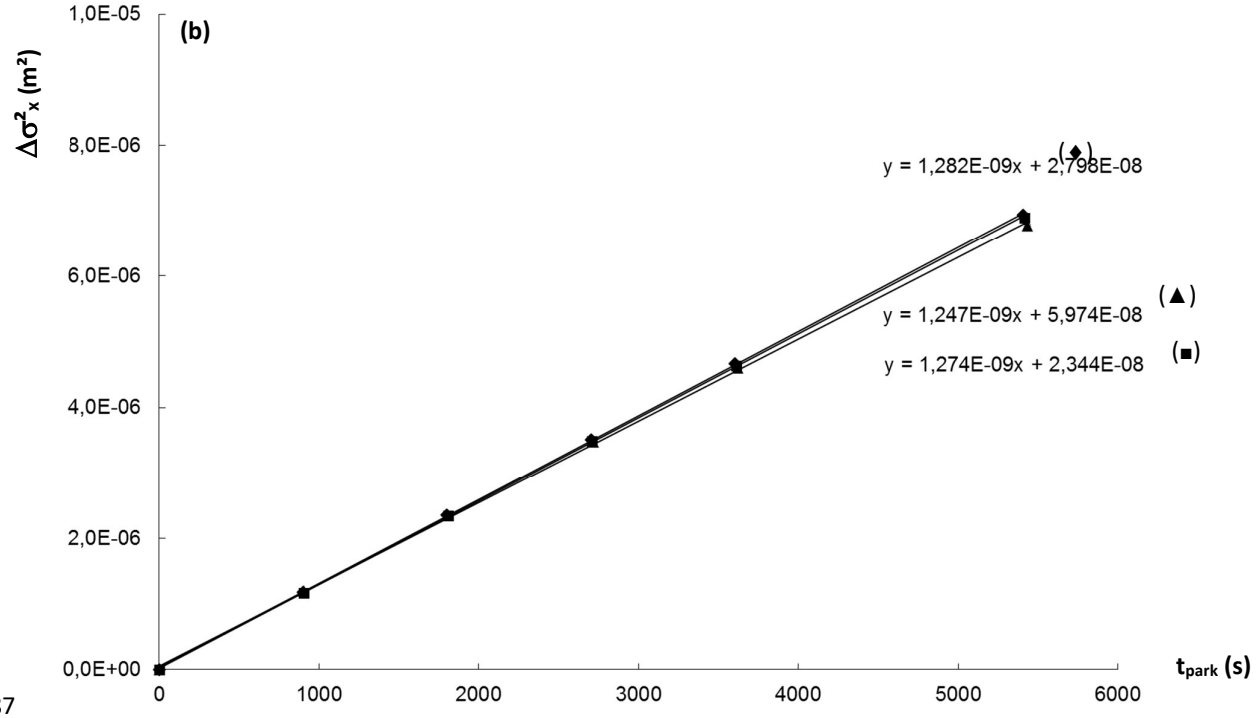

887

888 **Figure S-2:** Curves of $\Delta\sigma_x^2/(2 \cdot t_{park})$ versus t_{park} for **(a)** acetophenone and **(b)** 3'-
889 methylacetophenone on (♦) an Infinity 1290 UHPLC instrument on day 1, (▲) an
890 Infinity 1290 UHPLC instrument on day 2, and (■) an Ultimate 3000 HPLC instrument
891 on day 3. Error bars indicate the standard variations obtained by performing the same
892 experiment four times consecutively. Data analyzed at half the peak height.

893

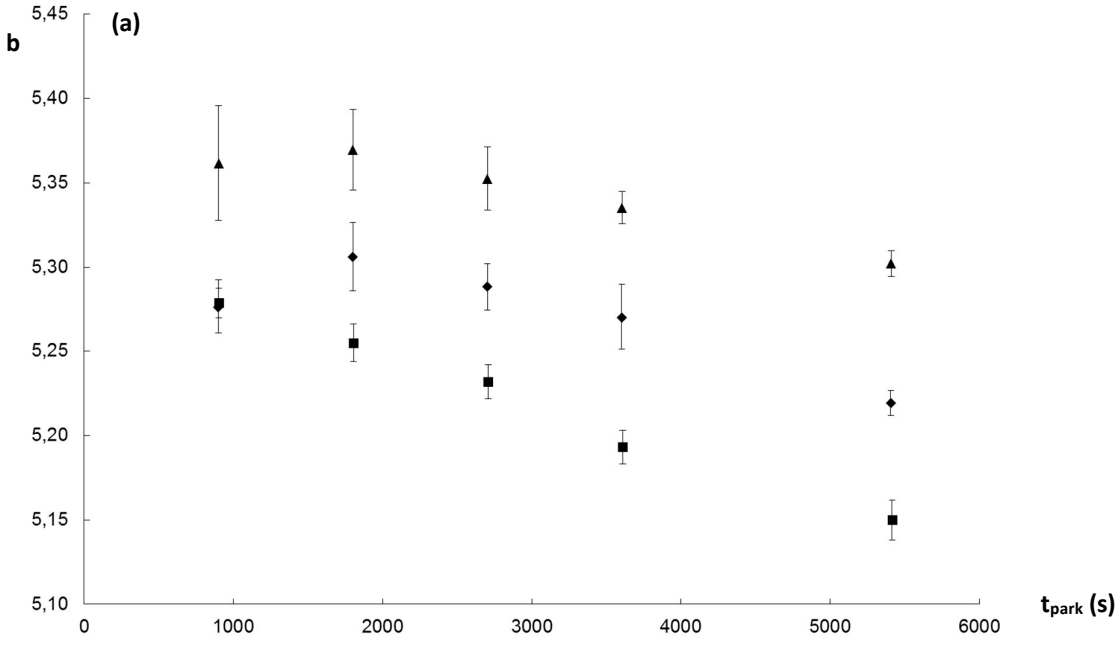

894

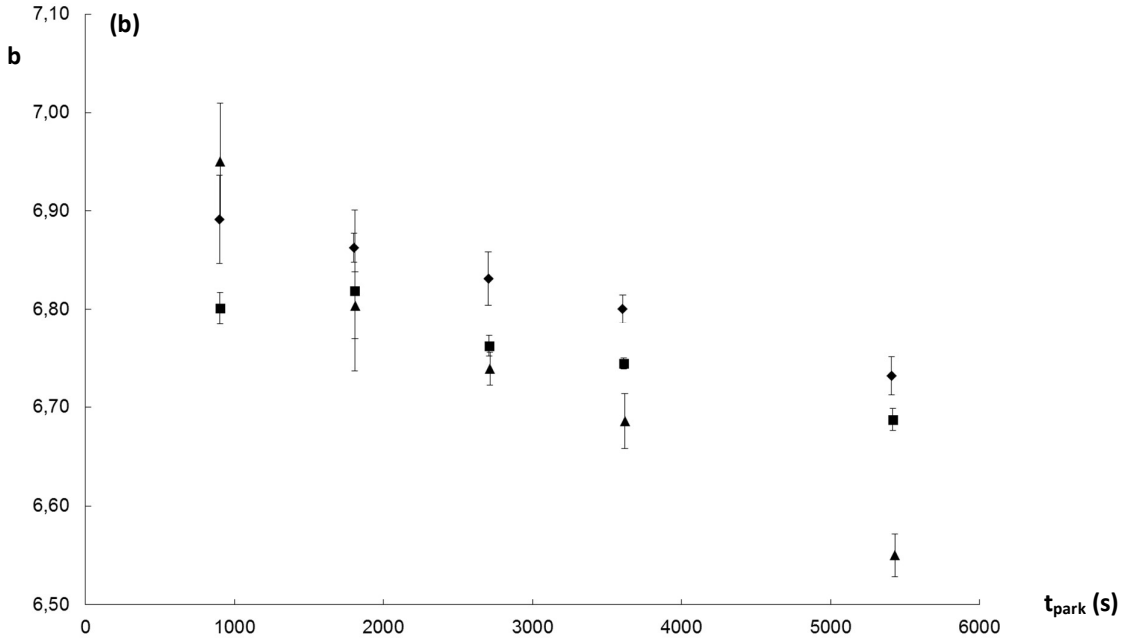

Figure S-3: Curves of plate height (H) versus interstitial velocity (u_i) for **(a)** acetophenone and **(b)** 3'-methylacetophenone. The displayed data are the average values obtained for three measurements on three different days. Standard deviations on these values are shown as error bars. Data analyzed at half the peak height.

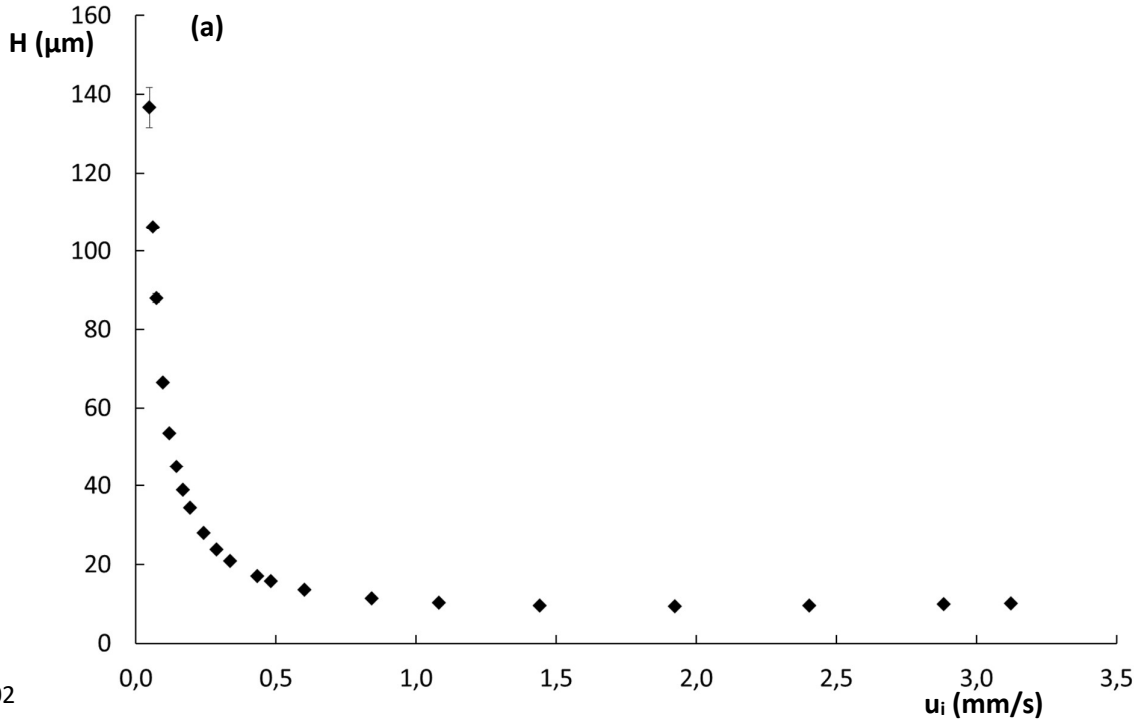

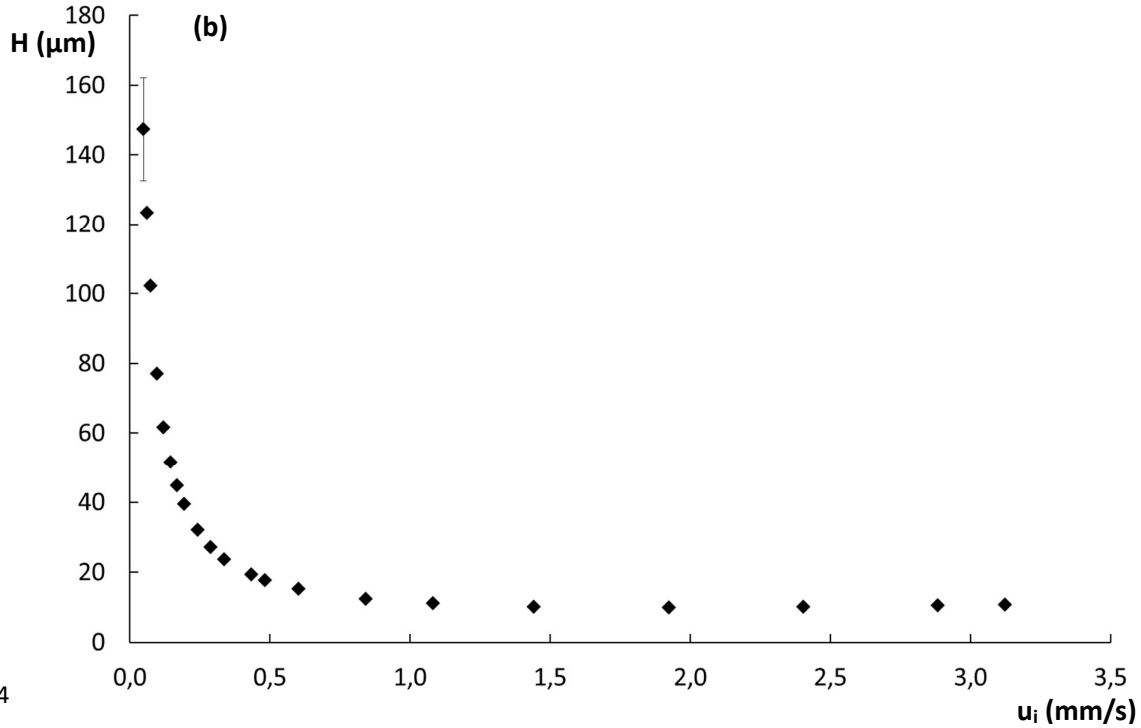

Figure S-4: Curves of $h \cdot \nu_i$ versus ν_i for acetophenone analyzed at half the peak height. The symbols indicate the raw plate height data, the lines are the fitted curves obtained by fitting the experimental data to one of following plate height models: ( ) van Deemter, ( ) Knox, ( ) free Knox, ( ) Giddings. The first two data points were omitted for the curve fitting.

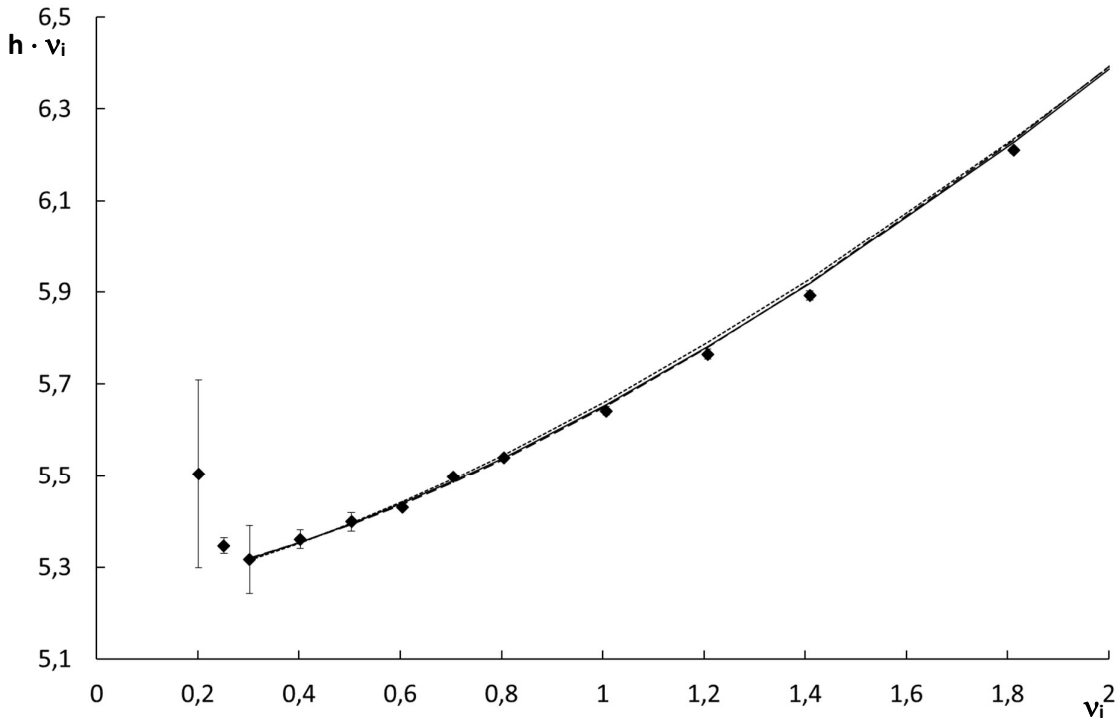

Figure S-5: Curves of $h \cdot \nu_i$ versus ν_i for (a) acetophenone and (b) 3'-methylacetophenone for experimental plate height data analyzed at half the peak height. Experimental plate height data were fitted using the free n-Knox model by omitting the first two datapoints ( ). The horizontal lines represent the b-term values obtained from the slope of the peak parking experiments ( ) and from the average of the individual peak parking data ( ). The b-term values obtained for the individual peak parking experiments are shown by the open symbols on the y-axis (◊ t_{park}= 15 min, ○ t_{park}= 30 min, □ t_{park}= 45 min, Δ t_{park}= 60 min and × t_{park}= 90 min).

933

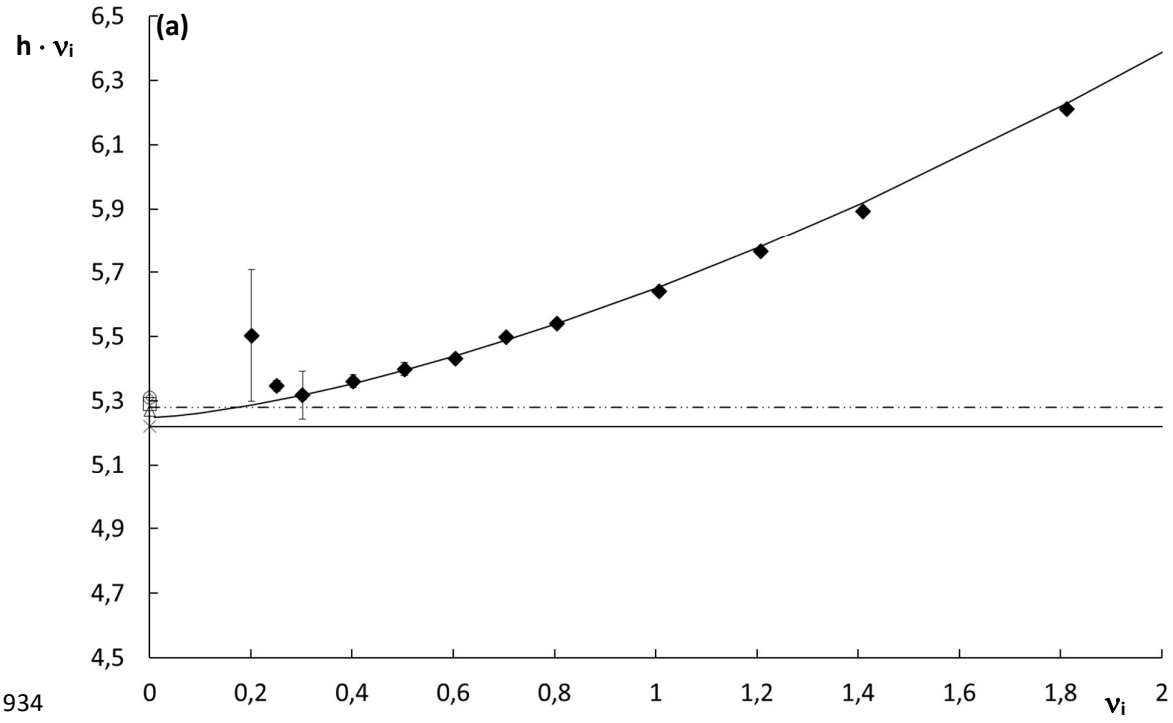

934

935

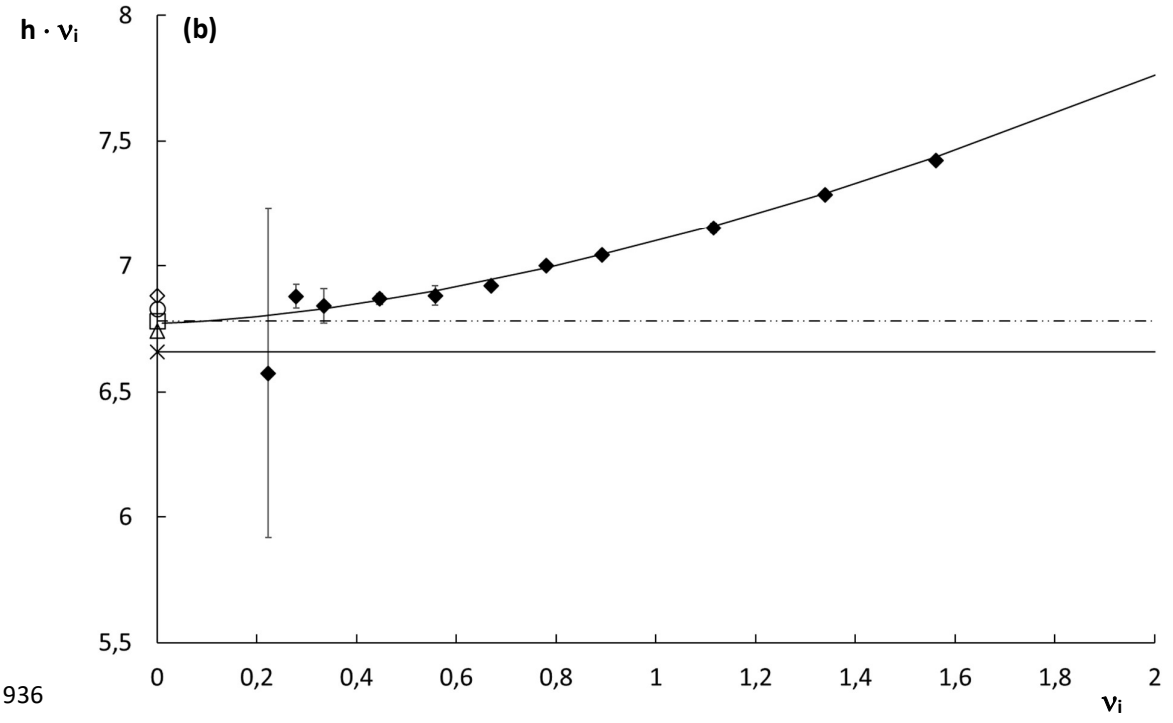

936

937

938